*Electronic Research Archive*

https://www.aimspress.com/journal/era

ERA, 33(10): 6241–6266.
DOI: 10.3934/era.2025276
Received: 17 September 2025
Revised: 13 October 2025
Accepted: 16 October 2025
Published: 22 October 2025

*Research article*

# A high accuracy method for the nonlinear fractional diffusion problem on network

**Yangming Zhang**[1] **and Yan Fan**[2,*]

[1] School of Mathematics and Statistics, Hunan First Normal University, Changsha 410006, China
[2] Xingzhi College, Zhejiang Normal University, Jinhua 321004, China

* **Correspondence:** Email: fanyan@zjnu.edu.cn.

**Abstract:** The fractional diffusion equation involving the fractional Laplacian is used to govern fractional random walk dynamics on network, which allowing long-range displacements. This paper develops a high accuracy numerical method for the computation of nonlinear fractional diffusion equation. The main idea is to approximate the spatial domain with a spectral Galerkin method based on Fourier-like basis functions, and then to discretize time by the general linear methods which contains Runge-Kutta methods, multistep methods, and many new classes of methods. For $(k, l)$-algebraically stable general linear methods with general stage order $p$, the nonlinear term satisfies the locally Lipschitz condition, and the proposed method is proved to be well-posed, stable, and convergent with order $p$ in time. Moreover, an optimal spatial error estimate is established, whose convergence rate is independent of the fractional parameter $\alpha$. Finally, several numerical experiments are presented to verify and support the theoretical results.

**Keywords:** network dynamics; fractional random walk; fractional diffusion; high accuracy numerical method; convergence and stability

## 1. Introduction

The dynamics of networks have broad applications in various fields of science and engineering, including real and digital social networks, traffic flow, epidemic propagation, human mobility, chemical reactions and computer systems [1–4]. The dynamical processes on networks, i.e., the strategy of a random walker moving between nodes, are of great importance. Normal random walks, where the walker jumps with equal probability from one node to its nearest neighbor, have been widely studied [5–7]. In contrast, fractional random walks, an extension of classical random walks inspired by Lévy flights, are used to describe random walks with long-range displacements on networks [8–10]. Fractional random walks are more efficient at navigating networks compared to traditional random

walks [11]. Generally, fractional random walks correspond to fractional diffusion processes on networks, which allow the dynamic incorporation of the small-world property by facilitating long-range connections [12].

In this work, we concentrate on the computational study of fractional diffusion on networks, with a particular focus on developing highly accurate methods for solving the nonlinear space fractional diffusion equation (NSFDE) in terms of

$$\begin{cases} \partial_t u(\boldsymbol{x},t) = -\nu(-\Delta)^{\frac{\alpha}{2}} u(\boldsymbol{x},t) + f(u(\boldsymbol{x},t),\boldsymbol{x},t),\ t\in(0,T],\ \boldsymbol{x}\in\Omega^d,\ \Omega=(-1,1), \\ u(\boldsymbol{x},0) = u_0(\boldsymbol{x}),\ \boldsymbol{x}\in\Omega^d, \\ \left(a_j^+ u(\boldsymbol{x},t) + b_j^+ \partial_{x_j} u(\boldsymbol{x},t)\right)|_{x_j=1} = 0 \text{ and } \left(a_j^- u(\boldsymbol{x},t) + b_j^- \partial_{x_j} u(\boldsymbol{x},t)\right)|_{x_j=-1} = 0, \end{cases} \tag{1.1}$$

where $\boldsymbol{x} = (x_1, x_2, \ldots, x_d)$, $\alpha \in (0,2)$, and $\nu > 0$ is diffusion coefficient. The operator $(-\Delta)^{\frac{\alpha}{2}}$ denotes space fractional Laplacian, which captures nonlocality in space, such as long-range displacements and superdiffusion. Another important case is the time-fractional derivative, which captures nonlocality in time, including memory, long waiting times, and subdiffusion [13, 14]. Numerical methods for fractional diffusion equations have received considerable attention in recent years and a lot of literature is available on this topic. For example, finite difference methods [15, 16], finite volume method [17], Monte Carlo methods [18, 19], fast algorithms [20], finite element methods [21–23] and spectral methods [24–27]. A main challenge of constructing numerical schemes for fractional differential equations is the nonlocality and singularity of fractional differential operators. According to the inherent properties of fractional differential operator, some researchers proposed a series of orthogonal basis functions, which can handle the nonlocal and singular nature of fractional differential operators. For example, the generalized Jacobi functions [28] for the Riemann-Liouville fractional differential operators, Fourier-like basis functions [29] for the spectral fractional Laplacian, the Fourier-like mapped chebyshev functions [30], nontensorial generalized Hermite functions [31], and Gaussian radial basis functions [32] for the integral fractional Laplacian. The spectral Galerkin methods by these orthogonal basis functions usually provide high accuracy, and diagonal mass, and stiff matrix, which is suitable for approximating the space of fractional diffusion equation. To establish high-order numerical methods for the space fractional diffusion equation, the remaining part is how to discretize the temporal component. Generally, Crank-Nicolson (second-order) and BDF methods (first-order) are the most frequently used methods [27, 33–36], but their low order restricts the global accuracy. A natural approach to this problem is to employ high-order methods, for instance the $k$-step ($k < 5$) BDF method [37] and Runge-Kutta method [38]. Here, we investigate a more general class of methods, i.e., the general linear method, which contains linear multistep methods, Runge-Kutta methods, hybrid methods and many new classes of methods that may overcome the limitations of linear multistep and Runge-Kutta methods [39].

For the $d$-dimensional NSFDE (1.1), we approximate the spatial domain by a spectral Galerkin method based on the Fourier-like basis, which yields a diagonal mass and a stiffness matrix. It provides a favorable condition for using the high-order method in time and solving high-dimensional problems. By discretizing the time by the general linear method, we propose a class methods that is high-order both in space and in time for (1.1). Comparing with the existing high-order spectral methods whose global accuracy is restricted by low temporal convergence order, our method has high-order global accuracy. We give the solvability of the numerical scheme when the nonlinear term fulfills the locally Lipschitz condition. Under the $(k,l)$-algebraic stability, we prove the proposed method is stable, and

its temporal convergence rate equal to the general stage order of general linear methods. In addition, we derive the error estimate is space, in which the convergence rate is optimal and independent of the fractional parameter $\alpha$.

The structure of this paper is as follows. Section 2 provides an overview of the general linear method and introduction of the discrete spectral fractional Laplacian. Section 3 presents the full discretization for NSFDE (1.1), which combines the spectral Galerkin approach with a general linear method. Section 4 presents the theoretical analysis of the method, addressing solvability, stability, and convergence. Section 5 gives numerical experiments to test the theoretical results. Section 6 concludes the paper.

## 2. Preliminaries

First, we introduce the general linear method and the discrete spectral fractional Laplacian. For an ordinary differential equation $\frac{\mathrm{d}}{\mathrm{d}t}y(t) = f(t, y(t)),\ t \in (0, T]$ with $y(t_0) = y_0$, applying the general linear method (GLM) (see [40, 41]), we obtain

$$Y_i^n = \tau \sum_{j=1}^{s} \mathfrak{C}_{ij}^{11} f(t_n + \mu_j \tau, Y_j^n) + \sum_{j=1}^{r} \mathfrak{C}_{ij}^{12} y_j^{n-1},\ i = 1, 2, \ldots, s, \tag{2.1a}$$

$$y_i^n = \tau \sum_{j=1}^{s} \mathfrak{C}_{ij}^{21} f(t_n + \mu_j \tau, Y_j^n) + \sum_{j=1}^{r} \mathfrak{C}_{ij}^{22} y_j^{n-1},\ i = 1, 2, \ldots, r, \tag{2.1b}$$

$$\xi^n = \sum_{j=1}^{r} \beta_j y_j^n,\ n = 1, 2, \ldots. \tag{2.1c}$$

where $\tau > 0$ is the step size, the coefficients $\mathfrak{C}_{ij}^{IJ}$ $(I, J = 1, 2)$ and $\beta_j$ are real constants, $Y^{n,i}$, $y^{n,i}$, and $\xi^n$ are approximations to $y(t_n + \mu_i\tau)$, $h_i(t_n + \nu_i\tau)$, and $y(t_n + \eta\tau)$, respectively, every $h_i(t_n + \nu_i\tau)$ stands for a piece of information about the true solution $y(t)$ and $t_n = n\tau$, $\mu_i$, $\nu_i$, $\eta > 0$ are some real constants.

In the following, we denote $\mathfrak{C}_{IJ} = \left(\mathfrak{C}_{ij}^{IJ}\right)$ $(I, J = 1, 2)$, and recall the definition of $(k, l)$-algebraic stability.

**Definition 2.1.** *(see [40, 42]) If there exists two real constants $k > 0$ and $l$, a symmetric positive definite matrix $G \in \mathbb{R}^{r\times r}$ and a real matrix $D = \mathrm{diag}(d_1, d_2, \ldots, d_s)$ with $d_i \geq 0$ for $i = 1, 2, \ldots s$, such that*

$$\Psi = \begin{pmatrix} kG - \mathfrak{C}_{22}^{\mathrm{T}} G \mathfrak{C}_{22} - l\mathfrak{C}_{12}^{T} D \mathfrak{C}_{12} & \mathfrak{C}_{12}^{\mathrm{T}} D - \mathfrak{C}_{22}^{\mathrm{T}} G \mathfrak{C}_{21} - l\mathfrak{C}_{12}^{T} D \mathfrak{C}_{11} \\ D\mathfrak{C}_{12} - \mathfrak{C}_{21}^{\mathrm{T}} G \mathfrak{C}_{22} - l\mathfrak{C}_{11}^{T} D \mathfrak{C}_{12} & D\mathfrak{C}_{11} + \mathfrak{C}_{11}^{\mathrm{T}} D - \mathfrak{C}_{21}^{\mathrm{T}} G \mathfrak{C}_{21} - l\mathfrak{C}_{11}^{T} D \mathfrak{C}_{11} \end{pmatrix},$$

*is nonnegative definite, then the general linear method is said to be $(k, l)$-algebraically stable. Specifically, the $(1, 0)$ case is referred to simply as algebraically stable.*

The spectral fractional Laplacian in NSFDE (1.1) is defined as

$$(-\Delta)^{\frac{\alpha}{2}} v(\boldsymbol{x}) = \sum_{\boldsymbol{n}\in\mathbb{N}^d} \tilde{v}_{\boldsymbol{n}} \lambda_{\boldsymbol{n}}^{\frac{\alpha}{2}} \phi_{\boldsymbol{n}}(\boldsymbol{x}),$$

where $\lambda_{\boldsymbol{n}}$ and $\phi_{\boldsymbol{n}}(\boldsymbol{x})$ are the eigenpairs of Laplacian $-\Delta$ with the same boundary condition as in (1.1), respectively. Here, we assume the coefficients in the boundary conditions of (1.1) satisfy $a_j^{\pm} \geq 0$, $a_j^+ b_j^+ \geq 0$, $a_j^- b_j^- \leq 0$, $(a_j^+)^2 + (b_j^+)^2 \neq 0$, and $(a_j^-)^2 + (b_j^-)^2 \neq 0$, which ensures the well-posedness of Eq (1.1).

Let $\{\phi_{N,j}(x)\}_{j=1}^{N}$ be the Fourier-like basis in [43], $\{\lambda_{N,j}(x)\}_{j=1}^{N}$ be the eigenvalues satisfying

$$\left\langle -\Delta\phi_{N,i}(x), \phi_{N,j}(x)\right\rangle_{L^2(\Omega^d)} = |\lambda_{N,i}|_1\delta_{i,j},\ \delta_{i,j} = \begin{cases} 1, & i = j \\ 0, & else \end{cases}, \tag{2.2}$$

and $\Phi_{N,\boldsymbol{m}}(\boldsymbol{x}) = \prod_{j=1}^{d}\phi_{N,n_j}(x_j)$ with $\boldsymbol{m} \in \Lambda_N = \{\boldsymbol{m} = (m_1, m_2, \cdots, m_d) : m_i = 0, \cdots, N-2 \text{ and } i = 1, \cdots, d\}$. Next, we present the definition of the discrete spectral fractional Laplacian.

**Definition 2.2** ( [29]). *The discrete fractional Laplacian $(-\Delta_N)^{\frac{\alpha}{2}}$ is given by*

$$(-\Delta_N)^{\frac{\alpha}{2}}u_N(\boldsymbol{x}) = \sum_{\boldsymbol{n}\in\Upsilon_N}\tilde{u}_{\boldsymbol{n}}|\lambda_{N,\boldsymbol{n}}|_1^{\frac{\alpha}{2}}\Phi_{N,\boldsymbol{n}}(\boldsymbol{x}), \forall u_N(\boldsymbol{x}) = \sum_{\boldsymbol{n}\in\Upsilon_N}\tilde{u}_{\boldsymbol{n}}\Phi_{N,\boldsymbol{n}}(\boldsymbol{x}) \in V_N^d. \tag{2.3}$$

*where $V_N^d = \text{span}\left\{\Phi_{N,\boldsymbol{n}}(\boldsymbol{x}) : \boldsymbol{n} \in \Lambda_N, \boldsymbol{x} \in \Omega^d\right\}$ and $|\lambda_{N,\boldsymbol{n}}|_1 = \lambda_{N,n_1} + \lambda_{N,n_2} + \cdots + \lambda_{N,n_d}$, $\delta_{\boldsymbol{nm}} = \prod_{j=1}^{d}\delta_{n_jm_j}$.*

## 3. A high accuracy numerical method

Applying the spectral Galerkin method constructed by the $d$-dimensional $\Phi_{N,\boldsymbol{n}}(\boldsymbol{x})$, we establish the spatial semi-discretization of NSFDE (1.1),

$$\begin{cases} \partial_t u_N(\boldsymbol{x}, t) = -\nu(-\Delta_N)^{\frac{\alpha}{2}}u_N(\boldsymbol{x}, t) + \Pi_N^0 f(u_N(\boldsymbol{x}, t), \boldsymbol{x}, t), \\ u_N(\boldsymbol{x}, 0) = \Pi_N^0 u_0(\boldsymbol{x}), \end{cases} \tag{3.1}$$

where the $L^2$-orthogonal projection operator $\Pi_N^0 : L^2(\Omega^d) \to V_N^d$ is given by

$$\left\langle \Pi_N^0 u - u, v_N\right\rangle_{L^2(\Omega^d)} = 0, \quad \forall v_N \in V_N^d.$$

**Remark 3.1.** *With Definition 2.2 and the orthogonal properties (2.2), it is easy to find that the stiff matrix $S = diag\left(|\lambda_{N,\boldsymbol{n}}|_1^{\frac{\alpha}{2}}\right)$ $(\boldsymbol{n} \in \Gamma_N)$ in (3.1) is a diagonal matrix and the mass matrix is identity matrix. This provides great advantage for the numerical method to compute the high-dimensional problem.*

Applying the general linear method (2.1a)–(2.1c) to (3.1), we obtain the full discretization of NSFDE (1.1),

$$\begin{aligned} U_N^{n,i} &= \tau\sum_{j=1}^{s}\mathfrak{C}_{ij}^{11}\mathcal{F}(U_N^{n,j}) + \sum_{j=1}^{r}\mathfrak{C}_{ij}^{12}u_N^{n-1,j},\ i = 1, 2, \ldots, s, \\ u_N^{n,i} &= \tau\sum_{j=1}^{s}\mathfrak{C}_{ij}^{21}\mathcal{F}(U_N^{n,j}) + \sum_{j=1}^{r}\mathfrak{C}_{ij}^{22}u_N^{n-1,j},\ i = 1, 2, \ldots, r, \\ \xi_N^n &= \sum_{j=1}^{r}\beta_j u_N^{n,j},\ n = 1, 2, \ldots, \end{aligned}$$

where $U_N^{n,i}$, $u_N^{n,i}$, and $\xi_N^n$ are the numerical approximations to $u(\boldsymbol{x}, t_n+\mu_i\tau)$, $H_i(\boldsymbol{x}, t_n+\nu_i\tau)$, and $u(\boldsymbol{x}, t_n+\eta\tau)$, respectively, $\mathcal{F}(U_N^{n,j}) = -\nu(-\Delta_N)^{\frac{\alpha}{2}}U_N^{n,j} + \Pi_N^0 f(U_N^{n,j}, \boldsymbol{x}, t)\big|_{t=t_n+\mu_j\tau}$, and each $H_i(\boldsymbol{x}, t_n + \nu_i\tau)$ stands for a part of the data related to the true solution $u(\boldsymbol{x}, t)$.

To simplify the notation, we rewrite the above numerical scheme in a compact form

$$U_N^n = \tau\mathfrak{C}_{11}\mathcal{F}(U_N^n) + \mathfrak{C}_{12}u_N^{n-1}, \tag{3.3a}$$
$$u_N^n = \tau\mathfrak{C}_{21}\mathcal{F}(U_N^n) + \mathfrak{C}_{22}u_N^{n-1}, \tag{3.3b}$$
$$\xi_N^n = \beta^{\mathrm{T}}u_N^n. \tag{3.3c}$$

where $U_N^n = \left(U_N^{n,1}, U_N^{n,2}, \ldots, U_N^{n,s}\right)^{\mathrm{T}}$, $u_N^n = \left(u_N^{n,1}, u_N^{n,2}, \ldots, u_N^{n,r}\right)^{\mathrm{T}}$, $\beta = (\beta_1, \beta_2, \ldots, \beta_r)^{\mathrm{T}}$, and $\mathcal{F}(U_N^n) = \left(\mathcal{F}(U_N^{n,1}), \mathcal{F}(U_N^{n,2}), \ldots, \mathcal{F}(U_N^{n,s})\right)^{\mathrm{T}}$.

## 4. Theoretical analysis of the numerical method

First, we introduce some notations and properties. Let $\langle\cdot,\cdot\rangle_{L^2(\Omega^d)}$ and $\|\cdot\|_{L^2(\Omega^d)}$ be the $L^2$ inner product and norm, $H^\vartheta(\Omega^d)$ ($\vartheta > 0$) be the Sobolev space with norm $\|\cdot\|_{H^\mu(\Omega^d)}$ and semi-norm $|\cdot|_{H^\vartheta(\Omega^d)}$, and $H_0^\vartheta(\Omega^d)$ be the closure of $C_0^\infty(\Omega^d)$ with respect to the norm $\|\cdot\|_{H^\vartheta(\Omega^d)}$.

**Lemma 4.1** (see (3.13) in [29]). *The continuous spectral fractional Laplacian $(-\Delta)^{\frac{\alpha}{2}}$ and the discrete spectral fractional Laplacian $(-\Delta_N)^{\frac{\alpha}{2}}$ satisfy*

$$\left\langle(-\Delta)^{\frac{\alpha}{2}}u, v\right\rangle_{L^2(\Omega^d)} = \left\langle(-\Delta)^{\frac{\alpha}{4}}u, (-\Delta)^{\frac{\alpha}{4}}v\right\rangle_{L^2(\Omega^d)}, \quad \forall u,\ v \in H_0^{\frac{\alpha}{2}}(\Omega^d),$$
$$\left\langle(-\Delta_N)^{\frac{\alpha}{2}}u_N, v_N\right\rangle_{L^2(\Omega^d)} = \left\langle(-\Delta_N)^{\frac{\alpha}{4}}u_N, (-\Delta_N)^{\frac{\alpha}{4}}v_N\right\rangle_{L^2(\Omega^d)}, \quad \forall u_N,\ v_N \in V_N^d.$$

*The bilinears satisfy the continuity and coercivity*

$$\left\langle(-\Delta)^{\frac{\alpha}{4}}u, (-\Delta)^{\frac{\alpha}{4}}v\right\rangle_{L^2(\Omega^d)} \le C_b\|u\|_{H^{\frac{\alpha}{2}}(\Omega^d)}\|v\|_{H^{\frac{\alpha}{2}}(\Omega^d)},$$
$$\left\langle(-\Delta)^{\frac{\alpha}{4}}u, (-\Delta)^{\frac{\alpha}{4}}u\right\rangle_{L^2(\Omega^d)} \ge C_b\|u\|^2_{H^{\frac{\alpha}{2}}(\Omega^d)},$$
$$\left\langle(-\Delta_N)^{\frac{\alpha}{4}}u_N, (-\Delta_N)^{\frac{\alpha}{4}}v_N\right\rangle_{L^2(\Omega^d)} \le C_b\|u_N\|_{H^{\frac{\alpha}{2}}(\Omega^d)}\|v_N\|_{H^{\frac{\alpha}{2}}(\Omega^d)},$$
$$\left\langle(-\Delta_N)^{\frac{\alpha}{4}}u_N, (-\Delta_N)^{\frac{\alpha}{4}}u_N\right\rangle_{L^2(\Omega^d)} \ge C_b\|u_N\|^2_{H^{\frac{\alpha}{2}}(\Omega^d)}.$$

**Lemma 4.2** (fractional Poincaré-Friedrichs inequality [44]). *For $u(x) \in H^{\frac{\alpha}{2}}(\Omega^d)$, we have*

$$\|u(x)\|^2_{L^2(\Omega^d)} \le C_p\|u(x)\|^2_{H^{\frac{\alpha}{2}}(\Omega^d)}, \tag{4.1}$$

*where $C_p > 0$ is a constant.*

Next, we introduce the locally Lipschitz condition of $f(u(\boldsymbol{x},t),\boldsymbol{x},t)$, which is important in the theoretical analysis of the numerical method. The $f(u(\boldsymbol{x},t),\boldsymbol{x},t)$ satisfies

$$\|f(u(\boldsymbol{x},t),\boldsymbol{x},t) - f(u(\boldsymbol{x},t),\boldsymbol{x},t)\|_{L^2(\Omega^d)} \le L\|u(\boldsymbol{x},t) - v(\boldsymbol{x},t)\|_{L^2(\Omega^d)}, \text{ for } \|u(\boldsymbol{x},t) - v(\boldsymbol{x},t)\|_{L^2(\Omega^d)} \le l_0, \tag{4.2}$$

where $l_0 > 0$ is a constant and $L > 0$ is the Lipschitz constant.

*4.1. Solvability*

Let $B = (b_{ij})_{i,j=1}^{k}$ be a symmetric and nonnegative definite matrix, $\lambda_{min}$ and $\lambda_{max}$ be the smallest and largest eigenvalue of $B$. We introduce

$$(\mathfrak{g}, \mathfrak{h})_B = \sum_{i,j=1}^{k} b_{ij} \langle \mathfrak{g}_i, \mathfrak{h}_j \rangle_{L^2(\Omega^d)}, \quad \|\mathfrak{h}\|_B = \sqrt{(\mathfrak{h}, \mathfrak{h})_B}, \tag{4.3}$$

where $\mathfrak{g} = (\mathfrak{g}_1, \mathfrak{g}_2, \ldots, \mathfrak{g}_k)^{\mathrm{T}}$ and $\mathfrak{h} = (\mathfrak{h}_1, \mathfrak{h}_2, \ldots, \mathfrak{h}_k)^{\mathrm{T}}$, $g_i$ and $\mathfrak{h}_i \in L^2(\Omega^d)$ for $i = 1, 2, \ldots, k$. For the identity matrix $I$, we denote $(\cdot, \cdot)_I$ and $\|\cdot\|_I$ by $(\cdot, \cdot)$ and $\|\cdot\|$ for short.

**Definition 4.1** (coercively of $\mathfrak{C}_{11}$ [45])**.** *If there exists a positive definite matrix $D = diag(d_1, d_2, \ldots, d_s)$, $\kappa$ is the largest positive number that satisfies*

$$\left(\mathfrak{C}_{11}^{-1}\mathfrak{h}, \mathfrak{h}\right)_D \geq \kappa(\mathfrak{h}, \mathfrak{h})_D, \tag{4.4}$$

*where $\mathfrak{h} = (\mathfrak{h}_1, \mathfrak{h}_2, \ldots, \mathfrak{h}_s)$ with $\mathfrak{h}_i \in L^2(\Omega^d)$ $(i = 1, 2, \ldots, s)$.*

**Theorem 4.1** (Solvability)**.** *If the coefficient matrix $\mathfrak{C}_{11}$ is invertible and satisfies the coercivity (4.4), $f(u(\boldsymbol{x}, t), \boldsymbol{x}, t)$ satisfies the locally Lipschitz condition (4.2), and $\tau\left(L - \nu\frac{C_b}{C_p}\right) < \kappa_0$, $\kappa_0 = \sup_D\{\kappa\}$, and $\kappa$ is given in Definition 4.1, then for (3.3a), there exists a unique solution.*

*Proof.* From (3.3a), we have

$$\langle \mathcal{F}(u_N) - \mathcal{F}(v_N), u_N - v_N \rangle_{L^2(\Omega^d)} = \left\langle \nu(-\Delta_N)^{\frac{\alpha}{2}}(u_N - v_N) + f(u_N, \boldsymbol{x}, t) - f(v_N, \boldsymbol{x}, t), u_N - v_N \right\rangle_{L^2(\Omega^d)}.$$

Using Lemmas 4.1 and 4.2, locally Lipschitz condition (4.2), we obtain

$$\langle \mathcal{F}(u_N) - \mathcal{F}(v_N), u_N - v_N \rangle_{L^2(\Omega^d)} \leq \left(L - \nu\frac{C_b}{C_p}\right) \|u_N - v_N\|_{L^2(\Omega^d)}.$$

By $\tau\left(L - \frac{C_b}{C_p}\right) < \kappa_0$ and Theorem 9.16 in [45], (3.3a) exists a unique solution.

*4.2. Stability*

We introduce a perturbed problem as follows:

$$W_N^n = \tau\mathfrak{C}_{11}\left[\mathcal{F}(W_N^n) + b_n\right] + \mathfrak{C}_{12}w_N^{n-1}, \tag{4.5a}$$
$$w_N^n = \tau\mathfrak{C}_{21}\left[\mathcal{F}(W_N^n) + b_n\right] + \mathfrak{C}_{22}w_N^{n-1}, \tag{4.5b}$$

where $w_N^0 = u_N^0 + b_0$, $b_0, b_1, \cdots, b_r$ are the perturbations.

**Theorem 4.2** (Stability)**.** *For $k \in (0, 1]$, if $\mathfrak{C}_{11}$ satisfies (4.4), $f(u(\boldsymbol{x}, t), \boldsymbol{x}, t)$ satisfies (4.2), GLM (2.1a)–(2.1c) satisfies the $(k, l)$-algebraically stability, and $-2\tau\nu\frac{C_b}{C_p} \leq l$, then the numerical method (3.3a)–(3.3c) is stable.*

*Proof.* Subtracting the perturbed problems (4.5a) and (4.5b) from the numerical methods (3.3a) and (3.3b), we have

$$U_N^n - W_N^n = \tau\mathfrak{C}_{11}\left[\mathcal{F}(U_N^n) - \mathcal{F}(W_N^n) - b_n\right] + \mathfrak{C}_{12}(u_N^{n-1} - w_N^{n-1}), \tag{4.6a}$$
$$u_N^n - w_N^n = \tau\mathfrak{C}_{21}\left[\mathcal{F}(U_N^n) - \mathcal{F}(W_N^n) - b_n\right] + \mathfrak{C}_{22}(u_N^{n-1} - w_N^{n-1}). \tag{4.6b}$$

The general linear method satisfies $(k, l)$-algebraically stability, thus we obtain

$$\begin{aligned}&\|u_N^n - w_N^n\|_G^2 - k\|u_N^{n-1} - w_N^{n-1}\|_G^2 - 2\left(U_N^n - W_N^n, \tau(\mathcal{F}(U_N^n) - \mathcal{F}(W_N^n) - b_n)\right)_D + 2l\|U_N^n - W_N^n\|_D^2\\ &= -\left(\boldsymbol{\varphi_n}, \Psi\boldsymbol{\varphi_n}\right) \le 0,\end{aligned}$$

where $\boldsymbol{\varphi_n} = \begin{pmatrix} u_N^{n-1} - w_N^{n-1} \\ \tau(F(U_N^n) - F(W_N^n) - b_n) \end{pmatrix}$. Then, we arrive at

$$\|u_N^n - w_N^n\|_G^2 \le k\|u_N^{n-1} - w_N^{n-1}\|_G^2 + 2\left(U_N^n - W_N^n, \tau(\mathcal{F}(U_N^n) - \mathcal{F}(W_N^n) - b_n)\right)_D - 2l\|U_N^n - W_N^n\|_D^2. \tag{4.7}$$

By Lemmas 4.1 and 4.2, the locally Lipschitz condition (4.2), and $-2\tau\nu\frac{C_b}{C_p} \le l$, we arrive at

$$\begin{aligned}\|u_N^n - w_N^n\|_G^2 &\le k\|u_N^{n-1} - w_N^{n-1}\|_G^2 + (-2\tau\nu\frac{C_b}{C_p} - l)\|U_N^n - W_N^n\|_D^2 + (2L+1)\tau\|U_N^n - W_N^n\|_D^2 + \tau\|b_n\|_D\\ &\le k\|u_N^{n-1} - w_N^{n-1}\|_G^2 + (2L+1)\tau\|U_N^n - W_N^n\|_D^2 + \tau\|b_n\|_D.\end{aligned} \tag{4.8}$$

Next, we give an estimate of $\|U_N^n - W_N^n\|_D^2$, which is important in the proof of stability. From (4.6a), we have

$$\mathfrak{C}_{11}^{-1}(U_N^n - W_N^n) = \tau\left[\mathcal{F}(U_N^n) - \mathcal{F}(W_N^n) - b_n\right] + \mathfrak{C}_{11}^{-1}\mathfrak{C}_{12}(u_N^{n-1} - w_N^{n-1}).$$

Taking the inner product with $U_N^n - W_N^n$, we have

$$\begin{aligned}&\left(\mathfrak{C}_{11}^{-1}(U_N^n - W_N^n), U_N^n - W_N^n\right)_D - \left(\tau\left[\mathcal{F}(U_N^n) - \mathcal{F}(W_N^n)\right], U_N^n - W_N^n\right)_D\\ &\quad = -\tau\left(b_n, U_N^n - W_N^n\right)_D + \left(\mathfrak{C}_{11}^{-1}\mathfrak{C}_{12}(u_N^{n-1} - w_N^{n-1}), U_N^n - W_N^n\right)_D.\end{aligned} \tag{4.9}$$

Using (4.4), i.e., the coercivity of $\mathfrak{C}_{11}$, Lemmas 4.1 and 4.2, and the locally Lipschitz condition (4.2), we obtain

$$\begin{aligned}&\left(\kappa - \tau\left(L - \nu\frac{C_b}{C_p}\right)\right)\left\|U_N^n - W_N^n\right\|_D\\ &\le \left(\mathfrak{C}_{11}^{-1}(U_N^n - W_N^n), U_N^n - W_N^n\right)_D - \left(\tau\left[\mathcal{F}(U_N^n) - \mathcal{F}(W_N^n)\right], U_N^n - W_N^n\right)_D,\end{aligned}$$

where we employ a proper $D$ and $\tau$ such that $\left(\kappa - \tau\left(L - \nu\frac{C_b}{C_p}\right)\right) > 0$. For

$$\begin{aligned}&-\tau\left(b_n, U_N^n - W_N^n\right)_D + \left(\mathfrak{C}_{11}^{-1}\mathfrak{C}_{12}(u_N^{n-1} - w_N^{n-1}), U_N^n - W_N^n\right)_D\\ &\le \frac{1}{\epsilon}\left\|D^{\frac{1}{2}}\mathfrak{C}_{11}^{-1}\mathfrak{C}_{12}G^{-\frac{1}{2}}\right\|_2^2\left\|u_N^{n-1} - w_N^{n-1}\right\|_G^2 + (\tau+1)\,\epsilon\|U_N^n - W_N^n\|_D^2 + \frac{\tau}{\epsilon}\|b_n\|_D^2,\end{aligned}$$

with suitable $\epsilon$, and taking the above two inequalities into (4.9), we obtain

$$\|U_N^n - W_N^n\|_D^2 \le C_t \left[\|u_N^{n-1} - w_N^{n-1}\|_D^2 + \tau\|b_n\|_D^2\right]. \tag{4.10}$$

Substituting (4.10) into (4.8), by iteration, we have

$$\begin{aligned}\|u_N^n - w_N^n\|_G^2 \le& k\|u_N^{n-1} - w_N^{n-1}\|_G^2 + (2L+1)\tau C_t \left[\|u_N^{n-1} - w_N^{n-1}\|_D^2 + \tau\|b_n\|_D^2\right] + \tau\|b_n\|_D \\ \le& k^n\|u_N^0 - w_N^0\|_G^2 + (2L+1)\tau C_t \sum_{i=1}^{n} k^{n-i}\|u_N^{n-1} - w_N^{n-1}\|_D^2 \\ &+ ((2L+1)\tau C_t + 1)\sum_{i=1}^{n} k^{n-i}\|b_n\|_D.\end{aligned}$$

Using the discrete Grönwall inequality, we obtain

$$\|u_N^n - w_N^n\|_G^2 \le \exp((2L+1)C_t n\tau)\left[\|b_0\|_D + ((2L+1)\tau C_t + 1)\sum_{i=1}^{n} k^{n-i}\|b_n\|_D\right].$$

Then, the numerical method (3.3a)–(3.3c) is said to be stable.

### *4.3. Convergence*

To derive the convergence, we introduce the important $H^{\frac{\alpha}{2}}$-orthogonal projection operator $\prod_N^\alpha : H_0^{\frac{\alpha}{2}}(\Omega^d) \to V_N^d$, which is defined as

$$\left\langle (-\Delta)^{\frac{\alpha}{2}} u(\boldsymbol{x}), v_N \right\rangle_{L^2(\Omega^d)} = \left\langle (-\Delta)^{\frac{\alpha}{2}} \Pi_N^\alpha u(\boldsymbol{x}), v_N \right\rangle_{L^2(\Omega^d)}, \quad \forall\ v_N \in V_N^d. \tag{4.11}$$

In the following, we give the estimate of the operator $\Pi_N^\alpha$.

**Lemma 4.3** (see [38]). *For $v(\boldsymbol{x}) \in H_0^{\frac{\alpha}{2}}(\Omega^d) \cap H^m(\Omega^d)$, $m \ge \frac{\alpha}{2}$, we have*

$$\left\|v(\boldsymbol{x}) - \Pi_N^\alpha v(\boldsymbol{x})\right\|_{H^{\frac{\alpha}{2}}(\Omega^d)} \le C_2 N^{\frac{\alpha}{2}-m}\|v(\boldsymbol{x})\|_{H^m(\Omega^d)}, \tag{4.12}$$

$$\left\|v(\boldsymbol{x}) - \Pi_N^\alpha v(\boldsymbol{x})\right\|_{L^2(\Omega^d)} \le C_2 N^{-m}\|v(\boldsymbol{x})\|_{H^m(\Omega^d)}, \tag{4.13}$$

*where $C_2 > 0$ is a constant independent of $N$.*

For $\hat{u}_N(\boldsymbol{x}, t) = \Pi_N^\alpha u(\boldsymbol{x}, t)$, we have

$$\partial_t \hat{u}_N(\boldsymbol{x}, t) = -\nu(-\Delta)^{\frac{\alpha}{2}} \hat{u}_N(\boldsymbol{x}, t) + \Pi_N^0 f(\hat{u}(\boldsymbol{x}, t), \boldsymbol{x}, t) + Q(\boldsymbol{x}, t). \tag{4.14}$$

Here, $Q(\boldsymbol{x}, t) \in L^2\left(0, T; V_N^d\right)$ is a residual, which satisfies

$$\langle Q(\boldsymbol{x}, t), v_N\rangle_{L^2(\Omega^d)} = \langle \partial_t\left[\hat{u}_N(\boldsymbol{x}, t) - u(\boldsymbol{x}, t)\right] - \left[f(\hat{u}(\boldsymbol{x}, t), \boldsymbol{x}, t) - f(u(\boldsymbol{x}, t), \boldsymbol{x}, t)\right], v_N\rangle_{L^2(\Omega^d)}. \tag{4.15}$$

Then, (4.15) is obtained by subtracting (1.1) from (4.14).

**Definition 4.2** (see [41, 42]). *The GLM (3.3) is said to have generalized stage order m, if $m \in \mathbb{N}$ is the maximal number fulfills the following conditions:*

*There exists an abstract function*

$$\tilde{H}(\boldsymbol{x}, t_n) = \left(\tilde{H}_1(\boldsymbol{x}, t_n + \nu_1\tau), \tilde{H}_2(\boldsymbol{x}, t_n + \nu_2\tau), \cdots, \tilde{H}_r(\boldsymbol{x}, t_n + \nu_r\tau)\right)^T,$$

*satisfying*

$$\left\|\tilde{H}(\boldsymbol{x}, t_n) - \hat{H}(\boldsymbol{x}, t_n)\right\| \le C_3\tau^m \left\|\partial_t^m \hat{u}_N(\boldsymbol{x}, t_n)\right\|_{L^2(\Omega^d)} \le C_3\tau^m \left\|\partial_t^m u(\boldsymbol{x}, t_n)\right\|_{H^{\frac{\alpha}{2}}(\Omega^d)}, \tag{4.16}$$

$$\|\delta^\tau(t_n)\| \le C_3\tau^{m+1} \sup_{\zeta\in[0,1]} \left\|\partial_t^{m+1} \hat{u}_N(\boldsymbol{x}, t_n+\zeta\tau)\right\|_{L^2(\Omega^d)} \le C_3\tau^{m+1} \sup_{\zeta\in[0,1]} \left\|\partial_t^{m+1} u(\boldsymbol{x}, t_n+\zeta\tau)\right\|_{H^{\frac{\alpha}{2}}(\Omega^d)}, \tag{4.17}$$

$$\|\theta^\tau(t_n)\| \le C_3\tau^{m+1} \sup_{\zeta\in[0,1]} \left\|\partial_t^{m+1} \hat{u}_N(\boldsymbol{x}, t_n+\zeta\tau)\right\|_{L^2(\Omega^d)} \le C_3\tau^{m+1} \sup_{\zeta\in[0,1]} \left\|\partial_t^{m+1} u(\boldsymbol{x}, t_n+\zeta\tau)\right\|_{H^{\frac{\alpha}{2}}(\Omega^d)}, \tag{4.18}$$

$$\|\sigma^\tau(t_n)\|_{L^2(\Omega^d)} \le C_3\tau^m \left\|\partial_t^m \hat{u}_N(\boldsymbol{x}, t_n)\right\|_{L^2(\Omega^d)} \le C_3\tau^m \left\|\partial_t^m u(\boldsymbol{x}, t_n)\right\|_{H^{\frac{\alpha}{2}}(\Omega^d)}, \tag{4.19}$$

*where* $\hat{H}(\boldsymbol{x}, t_n) = \left(\hat{H}_1(\boldsymbol{x}, t_n + \nu_1\tau), \hat{H}_2(\boldsymbol{x}, t_n + \nu_2\tau), \ldots, \hat{H}_r(\boldsymbol{x}, t_n + \nu_r\tau)\right)^{\mathrm{T}}$ *with* $\hat{H}_j(\boldsymbol{x}, t_n + \nu_i\tau) = \Pi_N^\alpha H_j(\boldsymbol{x}, t_n + \nu_j\tau)$, $\delta^\tau(t_n)$, $\tau \in (0, \tau_0]$, $\tau_0$ *is the maximum step size which satisfies* $\tau_0\mu_i$ *and* $\tau_0\nu_j \in (0, T]$, $\theta^\tau(t_n)$ *and* $\sigma^\tau(t_n)$ *are the defects of equation*

$$\hat{U}_N^n = \tau\mathfrak{C}_{11}\left[\hat{\mathcal{F}}(\hat{U}_N^n) + Q^n\right] + \mathfrak{C}_{12}\tilde{H}(\boldsymbol{x}, t_{n-1}) + \delta^\tau(t_{n-1}), \tag{4.20a}$$

$$\tilde{H}(\boldsymbol{x}, t_n) = \tau\mathfrak{C}_{21}\left[\hat{\mathcal{F}}(\hat{U}_N^n) + Q^n\right] + \mathfrak{C}_{22}\tilde{H}(\boldsymbol{x}, t_{n-1}) + \theta^\tau(t_{n-1}), \tag{4.20b}$$

$$\hat{u}(\boldsymbol{x}, t_n + \eta\tau) = \beta^{\mathrm{T}}\tilde{H}(\boldsymbol{x}, t_n) + \sigma^\tau(t_n), \tag{4.20c}$$

*with* $\hat{U}_N^n = \left(\hat{U}_N^{n,1}, \hat{U}_N^{n,2}, \cdots, \hat{U}_N^{n,s}\right)^T$, $\hat{U}_N^{n,i} = \hat{u}_N(\boldsymbol{x}, t_n + \mu_i\tau)$, $Q_n = (Q_{n,1}, Q_{n,2}, \cdots, Q_{n,s})^T$, $Q_{n,i} = Q(\boldsymbol{x}, t_n+\mu_i\tau)$, $\hat{\mathcal{F}}\left(\hat{U}_N^n\right) = \left(\hat{\mathcal{F}}\left(\hat{U}_N^{n,1}\right), \hat{\mathcal{F}}\left(\hat{U}_N^{n,2}\right), \cdots, \hat{\mathcal{F}}\left(\hat{U}_N^{n,s}\right)\right)^T$, $\hat{\mathcal{F}}(\hat{U}_N^{n,i}) = -\nu(-\Delta)^{\frac{\alpha}{2}}\hat{U}_N^{n,i} + \Pi_N^0 f(\hat{U}_N^{n,i}, \boldsymbol{x}, t)\big|_{t=t_n+\mu_i\tau}$, *and* $C_3 > 0$ *is a constant independent of N and* $\tau$. *In particular, if* $\hat{H}(\boldsymbol{x}, t) = \tilde{H}(\boldsymbol{x}, t)$, *the generalized stage order reduces to the stage order.*

For the next result, we consider a more general case, i.e., $(k, l, p)$-algebraic stability [42], where $(k, l, 0)$-algebraically stable method is called $(k, l)$-algebraically stable.

**Lemma 4.4.** *If the general linear method (2.1a)–(2.1c) is* $(k, l, p)$*-algebraically stale for G and D,* $k \in (0, 1]$, *then*

$$\boldsymbol{\Psi} = \begin{pmatrix} G - \mathfrak{C}_{22}^{\mathrm{T}} G\mathfrak{C}_{22} - l\mathfrak{C}_{12}^{\mathrm{T}}\boldsymbol{D}\mathfrak{C}_{12} & \mathfrak{C}_{12}^{\mathrm{T}}\boldsymbol{D} - \mathfrak{C}_{22}^{\mathrm{T}} G\mathfrak{C}_{21} - l\mathfrak{C}_{12}^{\mathrm{T}}\boldsymbol{D}\mathfrak{C}_{11} \\ \boldsymbol{D}\mathfrak{C}_{12} - \mathfrak{C}_{21}^{\mathrm{T}} G\mathfrak{C}_{22} - l\mathfrak{C}_{11}^{\mathrm{T}}\boldsymbol{D}\mathfrak{C}_{12} & \mathfrak{C}_{11}^{\mathrm{T}}\boldsymbol{D} + \boldsymbol{D}\mathfrak{C}_{11} - \mathfrak{C}_{21}^{\mathrm{T}} G\mathfrak{C}_{21} - l\mathfrak{C}_{11}^{\mathrm{T}}\boldsymbol{D}\mathfrak{C}_{11} - p\boldsymbol{D} \end{pmatrix}$$

*is a nonnegative definite matrix for any* $n \ge 1$, *where* $\boldsymbol{D}$=blockdiag$(D, D, \ldots, D) \in \mathbb{R}^{ns\times ns}$,

$$\mathfrak{C}_{11} = \begin{pmatrix} \mathfrak{C}_{11} & & & & \\ \mathfrak{C}_{12}\mathfrak{C}_{21} & \mathfrak{C}_{11} & & & \\ \mathfrak{C}_{12}\mathfrak{C}_{22}B_{21} & \mathfrak{C}_{12}\mathfrak{C}_{21} & \mathfrak{C}_{11} & & \\ \vdots & \vdots & \ddots & \ddots & \\ \mathfrak{C}_{12}\mathfrak{C}_{22}^{n-2}\mathfrak{C}_{21} & \mathfrak{C}_{12}\mathfrak{C}_{22}^{n-3}\mathfrak{C}_{21} & \cdots & \mathfrak{C}_{12}\mathfrak{C}_{21} & \mathfrak{C}_{11} \end{pmatrix} \in \mathbb{R}^{ns\times ns}, \quad \mathfrak{C}_{12} = \begin{pmatrix} \mathfrak{C}_{12} \\ \mathfrak{C}_{12}\mathfrak{C}_{22} \\ \mathfrak{C}_{12}\mathfrak{C}_{22}^2 \\ \vdots \\ \mathfrak{C}_{12}\mathfrak{C}_{22}^{n-1} \end{pmatrix} \in \mathbb{R}^{ns\times r},$$

$$\mathfrak{C}_{21} = \left(\mathfrak{C}_{22}^{n-1}\mathfrak{C}_{21}, \mathfrak{C}_{22}^{n-2}\mathfrak{C}_{21}, \ldots, \mathfrak{C}_{21}\right) \in \mathbb{R}^{r\times ns}, \quad \mathfrak{C}_{22} = \mathfrak{C}_{22}^n \in \mathbb{R}^{r\times r}.$$

*Proof.* We divide the matrix $\Psi$ in Definition 2.1 into three parts, i.e.,

$$\Psi = \Psi_1 + \Psi_2 + \Psi_3, \text{ where } \Psi_1 = \begin{pmatrix} kG - \mathfrak{C}_{22}^{\mathrm{T}} G \mathfrak{C}_{22} & \mathfrak{C}_{12}^{\mathrm{T}} D - \mathfrak{C}_{22}^{\mathrm{T}} G \mathfrak{C}_{21} \\ D\mathfrak{C}_{12} - \mathfrak{C}_{21}^{\mathrm{T}} G \mathfrak{C}_{22} & \mathfrak{C}_{11}^{\mathrm{T}} D + D\mathfrak{C}_{11} - \mathfrak{C}_{21}^{\mathrm{T}} G \mathfrak{C}_{21} \end{pmatrix},$$
$$\Psi_2 = \begin{pmatrix} -l\mathfrak{C}_{12}^{\mathrm{T}} D\mathfrak{C}_{12} & -l\mathfrak{C}_{12}^{\mathrm{T}} D\mathfrak{C}_{11} \\ -l\mathfrak{C}_{11}^{\mathrm{T}} D\mathfrak{C}_{12} & -l\mathfrak{C}_{11}^{\mathrm{T}} D\mathfrak{C}_{11} \end{pmatrix}, \qquad \Psi_3 = \begin{pmatrix} \mathbf{0} & \mathbf{0} \\ \mathbf{0} & -pD \end{pmatrix}, \text{ and } \Psi_0 = \begin{pmatrix} (1-k)G & \mathbf{0} \\ \mathbf{0} & \mathbf{0} \end{pmatrix}.$$

Let

$$\mathcal{B}_1 = \begin{pmatrix} I_r & \mathbf{0} & \mathbf{0} & \cdots & \mathbf{0} \\ \mathbf{0} & I_s & \mathbf{0} & \cdots & \mathbf{0} \end{pmatrix} \in \mathbb{R}^{(r+s)\times(r+ns)}$$
$$\mathcal{B}_i = \begin{pmatrix} \mathfrak{C}_{22}^{i-1} & \mathfrak{C}_{22}^{i-2}\mathfrak{C}_{21} & \cdots & \mathfrak{C}_{21} & \mathbf{0} & \mathbf{0} & \cdots & \mathbf{0} \\ \mathbf{0} & \mathbf{0} & \cdots & \mathbf{0} & I_s & \mathbf{0} & \cdots & \mathbf{0} \end{pmatrix} \in \mathbb{R}^{(r+s)\times(r+ns)}, \ i \geq 2.$$

From the proof of Lemma 3.1 in [46], we have

$$\sum_{i=1}^{n} \mathcal{B}_i^{\mathrm{T}} (\Psi_0 + \Psi_1) \mathcal{B}_i = \begin{pmatrix} G - \mathfrak{C}_{22}^{\mathrm{T}} G \mathfrak{C}_{22} & \mathfrak{C}_{12}^{\mathrm{T}} D - \mathfrak{C}_{22}^{\mathrm{T}} G \mathfrak{C}_{21} \\ D\mathfrak{C}_{12} - \mathfrak{C}_{21}^{\mathrm{T}} G \mathfrak{C}_{22} & \mathfrak{C}_{11}^{\mathrm{T}} D + D\mathfrak{C}_{11} - \mathfrak{C}_{21}^{\mathrm{T}} G \mathfrak{C}_{21} \end{pmatrix}$$

is a nonnegative definite matrix. For $\Psi_2$ and $\Psi_3$, we obtain

$$\sum_{i=1}^{n} \mathcal{B}_i^{\mathrm{T}} (\Psi_2 + \Psi_3) \mathcal{B}_i = \begin{pmatrix} -p\mathfrak{C}_{12}^{\mathrm{T}} D\mathfrak{C}_{12} & -l\mathfrak{C}_{12}^{\mathrm{T}} D\mathfrak{C}_{11} \\ -p\mathfrak{C}_{11}^{\mathrm{T}} D\mathfrak{C}_{12} & -l\mathfrak{C}_{11}^{\mathrm{T}} D\mathfrak{C}_{11} - pD \end{pmatrix}.$$

Combining the above two equalities, we have

$$\boldsymbol{\Psi} = \sum_{i=1}^{n} \mathcal{B}_i^{\mathrm{T}} (\Psi_0 + \Psi_1 + \Psi_2 + \Psi_3) \mathcal{B}_i.$$

Since the general linear method is $(k, l, p)$-algebraically stale, we have $\Psi = \Psi_1 + \Psi_2 + \Psi_3$ is nonnegative definite and $G$ is positive definite, which derive that $\boldsymbol{\Psi}$ is nonnegative definite.

**Theorem 4.3.** *Assume that $u(\boldsymbol{x}, t)$ and $\xi_N^n$ are given by NSFDE (1.1) and (3.3a)–(3.3c), respectively. If the coefficient matrix $\mathfrak{C}_{11}$ is invertible and satisfies (4.4), the spectral radius $\rho(\mathfrak{C}_{22} - \mathfrak{C}_{21}\mathfrak{C}_{11}^{-1}\mathfrak{C}_{12}) < 1$, GLM (2.1a)–(2.1c) with general stage order $p$ satisfies $(k, l)$-algebraically stability, $0 < k \leq 1$ and $-2\nu\tau C_2/C_p \leq l$, $\partial_t^p u(\boldsymbol{x}, t)$ and $\partial_t^{p+1} u(\boldsymbol{x}, t) \in L^\infty\left(0, T; H_0^{\frac{\alpha}{2}}(\Omega^d)\right)$, $u_0(\boldsymbol{x})$, and $\partial_t u(\boldsymbol{x}, t) \in H_0^{\frac{\alpha}{2}}(\Omega^d) \cap H^m(\Omega^d)$, then*

$$\begin{aligned} \left\| u(\boldsymbol{x}, t_n + \eta\tau) - \xi_N^n \right\|_{L^2(\Omega^d)}^2 \leq & C \left\{ \tau^{2p} \sup_{t\in[0,T]} \left[ \left\| \partial_t^p u(\boldsymbol{x}, t) \right\|_{H^{\frac{\alpha}{2}}(\Omega^d)}^2 + \left\| \partial_t^{p+1} u(\boldsymbol{x}, t) \right\|_{H^{\frac{\alpha}{2}}(\Omega^d)}^2 \right] \right. \\ & + N^{-2m} \left[ \|u_0(\boldsymbol{x})\|_{H^m(\Omega^d)}^2 + \int_0^T \|\partial_t u(\boldsymbol{x}, t)\|_{H^m(\Omega^d)}^2 \, \mathrm{d}t \right] \\ & \left. + \left\| H(\boldsymbol{x}, t_0) - u_N^0 \right\|_{H^{\frac{\alpha}{2}}(\Omega^d)}^2 \right\}, \end{aligned} \tag{4.21}$$

*where $C > 0$ is a constant that independent of $N$ and $\tau$, but depending on $T$, $C_b$ and $C_p$ are the constants in Lemmas 4.1 and 4.2, respectively.*

*Proof.* To derive the error estimate, we first consider an abstract problem

$$\tilde{U}_N^n = \tau\mathfrak{C}_{11}\left[\hat{F}\left(\tilde{U}_N^n\right) + Q^n\right] + \mathfrak{C}_{12}\tilde{u}_N^{n-1}, \tag{4.22a}$$

$$\tilde{u}_N^n = \tau\mathfrak{C}_{21}\left[\hat{F}\left(\tilde{U}_N^n\right) + Q^n\right] + \mathfrak{C}_{22}\tilde{u}_N^{n-1} + \theta^\tau(t_{n-1}), \tag{4.22b}$$

where $\tilde{u}_N^0 = \tilde{H}(\boldsymbol{x}, t_0)$. Subtracting (3.3a) and (3.3b) from (4.22a) and (4.22b), we arrive at

$$\begin{aligned}
\tilde{U}_N^n - U_N^n &= \tau\mathfrak{C}_{11}\left[\hat{F}\left(\tilde{U}_N^n\right) - F\left(U_N^n\right) + Q_n\right] + \mathfrak{C}_{12}(\tilde{u}_N^{n-1} - u_N^{n-1}),\\
\tilde{u}_N^n - u_N^n &= \tau\mathfrak{C}_{21}\left[\hat{F}\left(\tilde{U}_N^n\right) - F\left(U_N^n\right) + Q_n\right] + \mathfrak{C}_{22}(\tilde{u}_N^{n-1} - u_N^{n-1}) + \theta^\tau(t_{n-1}).
\end{aligned}$$

Similar to the derivation of (4.7) in Theorem 4.2, we obtain

$$\begin{aligned}
\left\|\tilde{u}_N^n - u_N^n - \theta^\tau(t_{n-1})\right\|_G^2 \le\, & k\left\|\tilde{u}_N^{n-1} - u_N^{n-1}\right\|_G^2 - 2l\left\|\tilde{U}_N^n - U_N^n\right\|_D^2\\
& + 2\left(\tilde{U}_N^n - U_N^n, \tau(-\nu(-\Delta)^{\frac{\alpha}{2}}\tilde{U}_N^n + \nu(-\Delta_N)^{\frac{\alpha}{2}}U_N^n + f(\tilde{U}_N^n, \boldsymbol{x}, t) - f(U_N^n, \boldsymbol{x}, t) + Q^n)\right)_D.
\end{aligned}$$

By Lemmas 4.1 and 4.2, the locally Lipschitz condition (4.2), $-2\tau\nu\frac{C_b}{C_p} \le l$, and (4.15), we arrive at

$$\begin{aligned}
\left\|\tilde{u}_N^n - u_N^n - \theta^\tau(t_{n-1})\right\|_G^2 \le\, & k\left\|\tilde{u}_N^{n-1} - u_N^{n-1}\right\|_G^2 + (2L+1)\tau\left\|\tilde{U}_N^n - U_N^n\right\|_D^2\\
& + \frac{\tau}{2}\left\|\partial_t\left(\hat{u}_N^n - u^n\right)\right\|_D^2 + \frac{\tau}{2}\left\|\hat{u}_N^n - u^n\right\|_D^2,
\end{aligned} \tag{4.24}$$

where $u^n = \left(u^{n,1}, u^{n,2}, \ldots, u^{n,s}\right)^{\mathrm{T}}$ and $u^{n,i} = u(\boldsymbol{x}, t_n + \mu_i\tau)$.

Similar to the derivation of (4.10) in Theorem 4.2, and by (4.4), we can obtain

$$\left\|\tilde{U}_N^n - U_N^n\right\|_D^2 \le C_1\left[\left\|\tilde{u}_N^{n-1} - u_N^{n-1}\right\|_G^2 + \tau\left\|\partial_t\left(\hat{u}_N^n - u^n\right)\right\|_D^2 + \tau\left\|\hat{u}_N^n - u^n\right\|_D^2\right],$$

Then, for (4.24), we have

$$\begin{aligned}
\left\|\tilde{u}_N^n - u_N^n\right\|_G^2 \le\, & k\left\|\tilde{u}_N^{n-1} - u_N^{n-1}\right\|_G^2 + (2L+1)\tau\left\|\tilde{u}_N^{n-1} - u_N^{n-1}\right\|_G^2 + \tau\left\|\tilde{u}_N^n - u_N^n\right\|_G^2\\
& + \left(\frac{1}{\tau} - 1\right)\|\theta^\tau(t_{n-1})\|_G^2 + \left((2L+1)\tau + \frac{1}{2}\right)\tau\left[\left\|\partial_t\left(\hat{u}_N^n - u^n\right)\right\|_D^2 + \left\|\hat{u}_N^n - u^n\right\|_D^2\right].
\end{aligned}$$

By iterating the above inequality, and then using the discrete Grönwall inequality, we obtain

$$\begin{aligned}
\left\|\tilde{u}_N^n - u_N^n\right\|_G^2 \le \exp(2(L+1)n\tau)\Bigg\{ & k^n\left\|\tilde{u}_N^0 - u_N^0\right\|_G^2 + \frac{1-\tau}{\tau}\sum_{i=1}^n k^{n-i}\|\theta^\tau(t_{i-1})\|_G^2\\
& + \left((2L+1)\tau + \frac{1}{2}\right)\sum_{i=1}^n k^{n-i}\left[\left\|\partial_t\left(\hat{u}_N^n - u^n\right)\right\|_D^2 + \left\|\hat{u}_N^n - u^n\right\|_D^2\right]\Bigg\}.
\end{aligned} \tag{4.25}$$

In the following, we give the estimate of $\|\tilde{H}(\boldsymbol{x}, t_n) - \tilde{u}_N^n\|_G$. Subtracting (4.20a) and (4.20b) from (4.22a) and (4.22b), we arrive at

$$\hat{U}_N^n - \tilde{U}_N^n = \tau\mathfrak{C}_{11}\left[\hat{F}\left(\hat{U}_N^n\right) - \tilde{F}\left(\hat{U}_N^n\right)\right] + \mathfrak{C}_{12}\left(\tilde{H}(\boldsymbol{x}, t_{n-1}) - \tilde{u}_N^{n-1} + \delta^\tau(t_{n-1})\right),$$

$$\tilde{H}(\boldsymbol{x}, t_n) - \tilde{u}_N^n = \tau \mathfrak{C}_{21} \left[ \hat{F}\left(\hat{U}_N^n\right) - \tilde{F}\left(\hat{U}_N^n\right) \right] + \mathfrak{C}_{22}\left(\tilde{H}(\boldsymbol{x}, t_{n-1}) - \tilde{u}_N^{n-1}\right).$$

With $\tilde{H}(\boldsymbol{x}, t_0) - \tilde{u}_N^0 = 0$, we study n steps simultaneously for the above equation, which yields

$$Z_n = \mathfrak{C}_{\mathbf{11}} P_n + \boldsymbol{\delta_n}, \tag{4.27a}$$

$$z_n = \mathfrak{C}_{\mathbf{21}} P_n, \tag{4.27b}$$

where $z_n = \tilde{H}(\boldsymbol{x}, t_n) - \tilde{u}_N^n$,

$$Z_n = \begin{pmatrix} \hat{U}_N^1 - \tilde{U}_N^1 \\ \hat{U}_N^2 - \tilde{U}_N^2 \\ \vdots \\ \hat{U}_N^n - \tilde{U}_N^n \end{pmatrix}, \quad P_n = \begin{pmatrix} \tau\left(\hat{F}(\hat{U}_N^1) - \hat{F}(\tilde{U}_N^1)\right) \\ \tau\left(\hat{F}(\hat{U}_N^2) - \hat{F}(\tilde{U}_N^2)\right) \\ \vdots \\ \tau\left(\hat{F}(\hat{U}_N^n) - \hat{F}(\tilde{U}_N^n)\right) \end{pmatrix}, \quad \boldsymbol{\delta_n} = \begin{pmatrix} \delta^\tau(t_0) \\ \delta^\tau(t_1) \\ \vdots \\ \delta^\tau(t_{n-1}) \end{pmatrix},$$

and $\mathfrak{C}_{\mathbf{11}}$ and $\mathfrak{C}_{\mathbf{21}}$ are defined in Lemma 4.4, i.e.,

$$\mathfrak{C}_{\mathbf{11}} = \begin{pmatrix} \mathfrak{C}_{11} & & & & \\ \mathfrak{C}_{12}\mathfrak{C}_{21} & \mathfrak{C}_{11} & & & \\ \mathfrak{C}_{12}\mathfrak{C}_{22}B_{21} & \mathfrak{C}_{12}\mathfrak{C}_{21} & \mathfrak{C}_{11} & & \\ \vdots & \vdots & \ddots & \ddots & \\ \mathfrak{C}_{12}\mathfrak{C}_{22}^{n-2}\mathfrak{C}_{21} & \mathfrak{C}_{12}\mathfrak{C}_{22}^{n-3}\mathfrak{C}_{21} & \cdots & \mathfrak{C}_{12}\mathfrak{C}_{21} & \mathfrak{C}_{11} \end{pmatrix} \in \mathbb{R}^{ns \times ns},$$

$$\mathfrak{C}_{\mathbf{21}} = \left(\mathfrak{C}_{22}^{n-1}\mathfrak{C}_{21}, \mathfrak{C}_{22}^{n-2}\mathfrak{C}_{21}, \ldots, \mathfrak{C}_{21}\right) \in \mathbb{R}^{r \times ns}.$$

By Lemma 4.4, we obtain

$$\|z_n\|_G^2 - 2\left(\mathfrak{C}_{\mathbf{11}} P_n, P_n\right)_{\boldsymbol{D}} + l\|\mathfrak{C}_{\mathbf{11}} P_n\|_{\boldsymbol{D}}^2 = -\left(\begin{pmatrix} \mathbf{0} \\ P_n \end{pmatrix}, \boldsymbol{\Psi}\begin{pmatrix} \mathbf{0} \\ P_n \end{pmatrix}\right) \leq 0.$$

With (4.27a), Lemmas 4.1 and 4.2, the locally Lipschitz condition (4.2), $-2\tau\nu\frac{C_b}{C_p} \leq l$, and (4.15), we arrive at

$$\begin{aligned} \|z_n\|_G^2 &\leq 2\left(\mathfrak{C}_{\mathbf{11}} P_n, P_n\right)_{\boldsymbol{D}} + l\|\mathfrak{C}_{\mathbf{11}} P_n\|_{\boldsymbol{D}}^2 \\ &\leq 2\left(Z_n - \boldsymbol{\delta_n}, P_n\right)_{\boldsymbol{D}} - l\|Z_n - \boldsymbol{\delta_n}\|_{\boldsymbol{D}}^2 \\ &\leq 2\tau L\|Z_n\|_{\boldsymbol{D}}^2 - 2\left(\boldsymbol{\delta_n}, \mathfrak{C}_{\mathbf{11}}^{-1}(Z_n - \boldsymbol{\delta_n})\right)_{\boldsymbol{D}} + 2l\left(Z_n, \boldsymbol{\delta_n}\right)_{\boldsymbol{D}} - l\|\boldsymbol{\delta_n}\|_{\boldsymbol{D}}^2 \\ &\leq 2\tau L\|Z_n\|_{\boldsymbol{D}}^2 + \|\boldsymbol{D}^{\frac{1}{2}}\mathfrak{C}_{\mathbf{11}}^{-1}\boldsymbol{D}^{-\frac{1}{2}}\|_2\left(\|Z_n\|_{\boldsymbol{D}} + 2|l|\,\|Z_n\|_{\boldsymbol{D}} - (l+1)\|\boldsymbol{\delta_n}\|_{\boldsymbol{D}}\right)\|\boldsymbol{\delta_n}\|_{\boldsymbol{D}}. \end{aligned}$$

Equation (3.18) in [46] shows that $\|\boldsymbol{D}^{\frac{1}{2}}\mathfrak{C}_{\mathbf{11}}^{-1}\boldsymbol{D}^{-\frac{1}{2}}\|_2$ is bounded. Next, we consider the estimate of $\|Z_n\|_{\boldsymbol{D}}$. Similar to the derivation of (4.10) in Theorem 4.2, and by (4.4), we have $\|Z_n\|_{\boldsymbol{D}}^2 \leq C_2\|\boldsymbol{\delta_n}\|_{\boldsymbol{D}}^2$. Then, we can derive that

$$\|z_n\|_{\boldsymbol{D}}^2 \leq C_3\|\boldsymbol{\delta_n}\|_{\boldsymbol{D}}^2. \tag{4.28}$$

Dividing $\hat{H}(\boldsymbol{x},t_n)-u_N^n$ to $\hat{H}(\boldsymbol{x},t_n)-\tilde{H}(\boldsymbol{x},t_n)+\tilde{H}(\boldsymbol{x},t_n)-\tilde{u}_N^n+\tilde{u}_N^n-u_N^n$. By Lemma 4.3, (4.16)–(4.18), (4.25) and (4.28), we can obtain

$$\begin{aligned}\|\hat{H}(\boldsymbol{x},t_n)-u_N^n\|_G^2 \le & C_4\left[\tau^{2p}\sup_{t\in[0,T]}\left(\left\|\partial_t^p u(\boldsymbol{x},t)\right\|^2_{H^{\frac{\alpha}{2}}(\Omega^d)}+\left\|\partial_t^{p+1}u(\boldsymbol{x},t)\right\|^2_{H^{\frac{\alpha}{2}}(\Omega^d)}\right)\right.\\ &\left.+N^{-2m}\left(\|u_0(\boldsymbol{x})\|^2_{H^m(\Omega^d)}+\int_0^T\|\partial_t u(\boldsymbol{x},t)\|^2_{H^m(\Omega^d)}\mathrm{d}t\right)+\left\|H(\boldsymbol{x},t_0)-u_N^0\right\|^2_{H^{\frac{\alpha}{2}}(\Omega^d)}\right].\end{aligned}$$

By (3.3c) and (4.20c), we arrive at

$$\begin{aligned}\left\|u(\boldsymbol{x},t_n+\eta\tau)-\xi_N^n\right\|^2_{L^2(\Omega^d)} \le & \left[\|u(\boldsymbol{x},t_n+\eta\tau)-\hat{u}_N(\boldsymbol{x},t_n+\eta\tau)\|_{L^2(\Omega^d)}+\left\|b^T(\tilde{H}(\boldsymbol{x},t_n)-\hat{H}(\boldsymbol{x},t_n))\right\|_{L^2(\Omega^d)}\right.\\ &\left.+\left\|b^T(\hat{H}(\boldsymbol{x},t_n)-u_N^n)\right\|_{L^2(\Omega^d)}+\|\sigma^\tau(t_n)\|_{L^2(\Omega^d)}\right]^2.\end{aligned}$$

Finally, by Lemma 4.3, (4.19) and $u(\boldsymbol{x},t)=u_0(\boldsymbol{x})+\int_0^t\frac{\partial}{\partial t}u(\boldsymbol{x},\zeta)\mathrm{d}\zeta$, we obtain (4.21).

**Remark 4.1.** *The domain $\Omega$ in (1.1) can be $\Omega=(a,b)$. Using a transformation $y=\frac{b-a}{2}x+\frac{b+a}{2}$, the domain $\Omega=(a,b)$ can transform to $(-1,1)$, Then, our theoretical results remain valid.*

## 5. Numerical experiment

Some numerical examples are provided in this section to validate the theoretical estimate in Theorem 4.3. The first example with nonsmooth exact solution is used to verify the convergence rates in space. The second example with smooth exact solution is to verify the convergence rate in time. For both examples, we consider three boundary conditions (Dirichlet BC, Neumann BC, Robin BC), and four general linear methods (i.e. multistep Runge-Kutta method with 4th-order (MRK-4) and 6th-order (MRK-6) [45,47,48], hybrid method with 4th-order (Hybrid-4) and with 5th-order (Hybrid-5) [42,49,50], which fulfill the conditions in Theorem 4.3. The third example illustrates the theoretical estimate for a 3-dimensional problem. The last example gives a numerical simulation for the fractional Allen-Cahn equation that is related to networks with long-range displacements. Since we focus on the spatial fractional order $\alpha\in(1,2)$, we take $\alpha=1.2$ and $\alpha=1.8$ to test the numerical method across the range of fractional behaviors. The value $\alpha=1.2$ represents strong long-range interactions, while $\alpha=1.8$ is close to the classical Laplacian.

**Example 5.1.** *We start with NSFDE (1.1) with* $u_0(\boldsymbol{x})=(-t_0)^z\left(1-x_1^2\right)^\xi\left(1-x_2^2\right)^\xi$,

$$\begin{aligned}f(u(\boldsymbol{x},t),\boldsymbol{x},t)=&z(t-t_0)^{z-1}\left(1-x_1^2\right)^\xi\left(1-x_2^2\right)^\xi+\nu(t-t_0)^z\sum_{i=0}^{\infty}\sum_{j=0}^{\infty}\hat{u}_{ij}\lambda_{ij}^{\frac{\alpha}{2}}\varphi_i(\boldsymbol{x})\varphi_j(\boldsymbol{x})\\ &+sin(u(\boldsymbol{x},t))-sin(t^z\left(1-x_1^2\right)^\xi\left(1-x_2^2\right)^\xi),\end{aligned}$$

*where $\lambda_{ij}=\lambda_i+\lambda_j$ and $\varphi_i(\boldsymbol{x})$ [51] are as follows*

**Dirichlet BC** $\lambda_n=\left(\frac{(n+1)\pi}{2}\right)^2$ *and* $\varphi_n(x)=\sin\left(\frac{(n+1)\pi(x+1)}{2}\right)$.

**Neumann BC** $\lambda_n=\left(\frac{n\pi}{2}\right)^2$ *and* $\varphi_n(x)=\cos\left(\frac{n\pi(x+1)}{2}\right)$.

**Robin BC** $\lambda_n = \left(\frac{\gamma_n}{2}\right)^2$ *and* $\varphi_n(x) = \sin\left(\frac{\gamma_n(x+1)}{2}\right) + \frac{\gamma_n}{2\kappa}\cos\left(\frac{\gamma_n(x+1)}{2}\right)$, *where* $\gamma_n$ *is the unique solve by*

$$\frac{\gamma_n}{\kappa}\cos(\gamma_n) + \left(1 - \left(\frac{\gamma_n}{2\kappa}\right)^2\right) sin(\gamma_n) = 0 \quad for \quad \gamma_n \in [(n-1)\pi, n\pi].$$

*The corresponding nonsmooth exact solution is* $u(\boldsymbol{x}, t) = (t - t_0)^z \left(1 - x_1^2\right)^\xi \left(1 - x_2^2\right)^\xi$.

For Example 5.1, Figures 1 and 2 give the plotting of exact solutions at the initial and final times. The errors and convergence rates in spaces for Example 5.1 are given in Figures 3–5. For a small number $\varepsilon$, $u(\boldsymbol{x}, t)$, $u_0(\boldsymbol{x}) \in L^2(0, T; H^{2\xi+0.5-\varepsilon}(\Omega^2))$. Theorem 4.3 predicts that the convergence rates in spaces are about 2.2 and 2.8 for $\xi = 0.85$ and $\xi = 1.15$, respectively, which is illustrated by the numerical results in Figures 3–5.

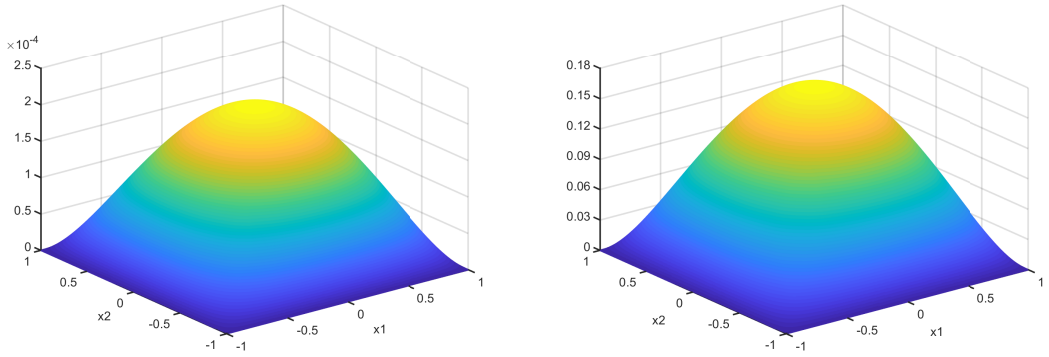


**(a)** $t = 0$ **(b)** $t = 1$

**Figure 1.** The plotting of exact solutions at the initial and final times for Example 5.1 with $z = 6.1$, and Dirichlet BC.

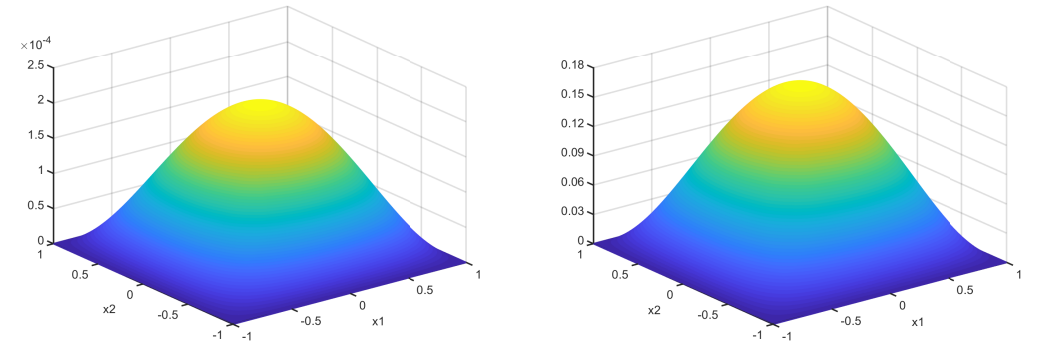


**(a)** $t = 0$ **(b)** $t = 1$

**Figure 2.** The plotting of exact solutions at the initial and final times for Example 5.1 with $z = 6.1$, Neumann BC, and Robin BC.

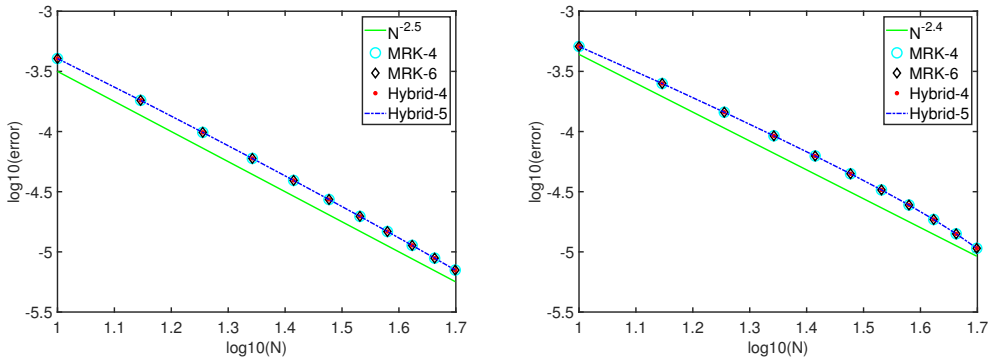


**(a)** $\alpha = 1.2$ **(b)** $\alpha = 1.8$

**Figure 3.** Errors and convergence rates in space for Example 5.1 with $z = 6.1$, $\nu = 0.3$, $t = 1$, $t_0 = 0.25$, $\xi = 0.85$, $\tau = \frac{1}{1000}$, and Dirichlet BC.

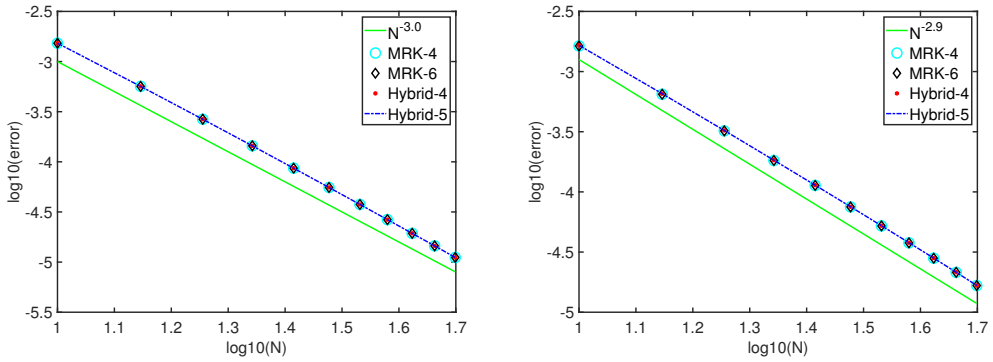


**(a)** $\alpha = 1.2$ **(b)** $\alpha = 1.8$

**Figure 4.** Errors and convergence rates in space for Example 5.1 with $z = 6.1$, $\nu = 0.2$, $t = 1$, $t_0 = 0.25$, $\xi = 1.15$, $\tau = \frac{1}{1000}$, and Neumann BC.

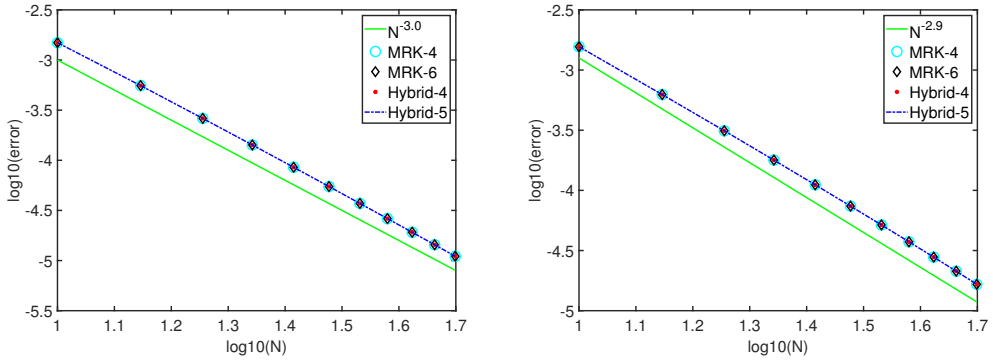


**(a)** $\alpha = 1.2$ **(b)** $\alpha = 1.8$

**Figure 5.** Errors and convergence rates in space for Example 5.1 with $z = 6.1$, $\nu = 0.1$, $t = 1$, $t_0 = 0.25$, $\xi = 1.15$, $\tau = \frac{1}{1000}$, and Robin BC.

**Example 5.2.** *We study the NSFDE (1.1) with $d = 2$ and three homogeneous boundary conditions as follows.*

**Dirichlet BC** *The NSFDE (1.1) with* $u_0(\boldsymbol{x}) = (-t_0)^z e^{-\frac{k_1 x_1^2}{1-x_1^2}-\frac{k_2 x_2^2}{1-x_2^2}}$,

$$f(u(\boldsymbol{x},t),\boldsymbol{x},t) = z(t-t_0)^{z-1}e^{-\frac{k_1 x_1^2}{1-x_1^2}-\frac{k_2 x_2^2}{1-x_2^2}} + \nu z(t-t_0)^z \sum_{i=0}^{\infty}\sum_{j=0}^{\infty} \hat{u}_{ij}\lambda_{ij}^{\frac{\alpha}{2}}\varphi_{ij}(\boldsymbol{x}) + \cos(u(\boldsymbol{x},t))$$
$$- \cos((t^2-t+0.25)^z e^{-\frac{k_1 x_1^2}{1-x_1^2}-\frac{k_2 x_2^2}{1-x_2^2}})$$

$\hat{u}_{ij} = \left\langle u(\boldsymbol{x},t), \varphi_{ij}(\boldsymbol{x})\right\rangle_{L^2(\Omega^2)}$, *$\varphi_{ij}(\boldsymbol{x})$ and $\lambda_{ij}$ are given in Example 5.1.*

*The corresponding exact solution is* $u(\boldsymbol{x},t) = (t-t_0)^z e^{-\frac{k_1 x_1^2}{1-x_1^2}-\frac{k_2 x_2^2}{1-x_2^2}}$

**Neumann BC** *The NSFDE (1.1) with* $u_0(\boldsymbol{x}) = (-t_0)^z \cos^3(\pi(x_1+1))\cos^3(\pi(x_2+1))$

$$f(u(\boldsymbol{x}),\boldsymbol{x},t) = z(t-t_0)^{z-1}\cos^3(\pi(x_1+1))\cos^3(\pi(x_2+1)) + \frac{\nu(t-t_0)^z}{16}\sum_{i=1}^{4}\lambda_i^{\frac{\alpha}{2}} w_i$$
$$+ u(\boldsymbol{x},t)^2 - (t-t_0)^{2z}\cos^6(\pi(x_1+1))\cos^6(\pi(x_2+1)).$$
$$w_1 = 9\cos(\pi(x_1+1))\cos(\pi(x_2+1)), \quad \lambda_1 = 2\pi^2,$$
$$w_2 = 3\cos(3\pi(x_1+1))\cos(\pi(x_2+1)), \quad \lambda_2 = 10\pi^2,$$
$$w_3 = 3\cos(\pi(x_1+1))\cos(3\pi(x_2+1)), \quad \lambda_3 = 10\pi^2,$$
$$w_4 = \cos(3\pi(x_1+1))\cos(3\pi(x_2+1)), \quad \lambda_4 = 18\pi^2.$$

*The corresponding exact solution is* $u(\boldsymbol{x},t) = (t-t_0)^z\cos^3(\pi(x_1+1))\cos^3(\pi(x_2+1))$.

**Robin BC** *The NSFDE (1.1) with boundary condition with* $b_1^- = -1$, $b_1^+ = a_1^- = a_2^+ = b_2^- = 0$ *and* $a_1^+ = a_2^- = b_2^+ = 1$, $u_0(\boldsymbol{x}) = \frac{1}{4^z}\phi(x_1)\phi(x_2)$, $u_0(\boldsymbol{x}) = (-t_0)^z\varphi(x_1)\varphi(x_2)$,

$$f(u(\boldsymbol{x}),\boldsymbol{x},t) = z(t-t_0)^{z-1}\varphi(x_1)\varphi(x_2) + \nu(\gamma^2/2)^{\alpha/2}(t-t_0)^z\varphi(x_1)\varphi(x_2), + u(\boldsymbol{x},t)^3$$
$$- (t-t_0)^{3z}\varphi(x_1)^3\varphi(x_2)^3.$$

*$\phi(x)$ and $\gamma$ are given in Example 5.1 with $n = 3$.*

*The corresponding exact solution is* $u(\boldsymbol{x},t) = (t-t_0)^z\varphi(x_1)\varphi(x_2)$.

For Example 5.2, Figures 6–8 give the plotting of exact solutions at the initial and final times. Let $rate = \ln\left(\frac{L^2-error(\tau)}{L^2-error(\tau/2)}\right)\Big/\ln 2$. The errors and convergence rates in time for Example 5.2 are presented in Tables 1–3 and Figures 9–11. With $z = 3.05$, we have $\partial_t^{p+1}u(\boldsymbol{x},t) \in L^1\left(0,T;H_0^{\frac{\alpha}{2}}(\Omega^d)\right)$ $(p = 4,5,6)$. As predicted by Theorem 4.3, the convergence rates in time for MRK4, MRK6, Hybrid-4 and Hybrid-5 are 4th 6th, 4th, and 5th, respectively, as verified by the numerical results in Tables 1–3. Since, the corresponding exact solution is smooth, we observe that the errors are decay exponentially in Figures 9–11, which confirm the estimate in Theorem 4.3.

**Table 1.** Errors and convergence rates in time for Example 5.2 with Dirichlet BC, $z = 6.1$, $\nu = \alpha^{-3}$, $N = 70$, $k_1 = k_2 = 20$, $t_0 = 0.5$, and $t = 1$.

| $\alpha$ | $\tau$ | MRK4 | | MRK6 | | Hybrid-4 | | Hybrid-5 | |
|---|---|---|---|---|---|---|---|---|---|
| | | $L^2$-error | rate | $L^2$-error | rate | $L^2$-error | rate | $L^2$-error | rate |
| | 1/16 | 3.3048E-06 | 3.8517 | 2.1243E-08 | 5.7845 | 9.1822E-07 | 3.9105 | 5.4810E-08 | 4.9357 |
| 1.2 | 1/32 | 2.2892E-07 | 3.9310 | 3.8540E-10 | 5.8930 | 6.1062E-08 | 3.9569 | 1.7909E-09 | 4.9694 |
| | 1/64 | 1.5009E-08 | 3.9669 | 6.4856E-12 | 5.9472 | 3.9321E-09 | 3.9789 | 5.7164E-11 | 4.9850 |
| | 1/128 | 9.5984E-10 | 3.9838 | 1.0511E-13 | 6.0118 | 2.4938E-10 | 3.9895 | 1.8050E-12 | 4.9906 |
| | 1/16 | 3.6933E-06 | 3.8245 | 3.2885E-08 | 5.7049 | 8.7507E-07 | 3.9039 | 5.2276E-08 | 4.9348 |
| 1.8 | 1/32 | 2.6070E-07 | 3.9182 | 6.3047E-10 | 5.8482 | 5.8460E-08 | 3.9535 | 1.7091E-09 | 4.9691 |
| | 1/64 | 1.7245E-08 | 3.9608 | 1.0944E-11 | 5.9229 | 3.7735E-09 | 3.9771 | 5.4569E-11 | 4.9849 |
| | 1/128 | 1.1075E-09 | 3.9809 | 1.8039E-13 | 5.9781 | 2.3961E-10 | 3.9887 | 1.7233E-12 | 4.9904 |

**Table 2.** Errors and convergence rates in time for Example 5.2 with Neumann BC, $z = 6.1$, $\nu = 2\alpha^{-4}$, $N = 50$, $t_0 = 0.55$, and $t = 1$.

| $\alpha$ | $\tau$ | MRK4 | | MRK6 | | Hybrid-4 | | Hybrid-5 | |
|---|---|---|---|---|---|---|---|---|---|
| | | $L^2$-error | rate | $L^2$-error | rate | $L^2$-error | rate | $L^2$-error | rate |
| | 1/16 | 7.7225E-06 | 3.8093 | 7.7301E-08 | 5.7130 | 1.8697E-06 | 3.8930 | 1.2616E-07 | 4.9243 |
| 1.2 | 1/32 | 5.5087E-07 | 3.9119 | 1.4737E-09 | 5.8566 | 1.2585E-07 | 3.9486 | 4.1549E-09 | 4.9644 |
| | 1/64 | 3.6596E-08 | 3.9580 | 2.5433E-11 | 5.9279 | 8.1511E-09 | 3.9748 | 1.3309E-10 | 4.9827 |
| | 1/128 | 2.3548E-09 | 3.9796 | 4.1776E-13 | 5.9428 | 5.1841E-10 | 3.9876 | 4.2091E-12 | 4.9926 |
| | 1/16 | 5.4847E-06 | 3.8188 | 5.0921E-08 | 5.7291 | 1.5545E-06 | 3.9015 | 9.2200E-08 | 4.9241 |
| 1.8 | 1/32 | 3.8867E-07 | 3.9162 | 9.6002E-10 | 5.8649 | 1.0402E-07 | 3.9524 | 3.0369E-09 | 4.9640 |
| | 1/64 | 2.5745E-08 | 3.9600 | 1.6473E-11 | 5.9319 | 6.7194E-09 | 3.9766 | 9.7299E-11 | 4.9825 |
| | 1/128 | 1.6543E-09 | 3.9805 | 2.6983E-13 | 5.9380 | 4.2683E-10 | 3.9884 | 3.0777E-12 | 4.9929 |

**Table 3.** Errors and convergence rates in time for Example 5.2 with Robin BC, $z = 6.1$, $\nu = \alpha^{-1}$, $N = 50$, $t_0 = 0.5$, and $t = 1$.

| $\alpha$ | $\tau$ | MRK4 | | MRK6 | | Hybrid-4 | | Hybrid-5 | |
|---|---|---|---|---|---|---|---|---|---|
| | | $L^2$-error | rate | $L^2$-error | rate | $L^2$-error | rate | $L^2$-error | rate |
| 1.2 | 1/8 | 1.2551E-03 | 3.7864 | 1.2579E-05 | 5.8589 | 5.7043E-04 | 3.8480 | 6.5276E-05 | 4.8630 |
| | 1/16 | 9.0966E-05 | 3.9040 | 2.1674E-07 | 5.9529 | 3.9614E-05 | 3.9286 | 2.2431E-06 | 4.9362 |
| | 1/32 | 6.0767E-06 | 3.9544 | 3.4988E-09 | 5.9826 | 2.6015E-06 | 3.9653 | 7.3265E-08 | 4.9691 |
| | 1/64 | 3.9198E-07 | 3.9778 | 5.5334E-11 | 5.9877 | 1.6655E-07 | 3.9829 | 2.3391E-09 | 4.9848 |
| 1.8 | 1/8 | 7.5398E-04 | 3.8424 | 3.9001E-06 | 6.1536 | 4.1583E-04 | 3.8553 | 4.1987E-05 | 4.8929 |
| | 1/16 | 5.2564E-05 | 3.9299 | 5.4785E-08 | 6.1582 | 2.8732E-05 | 3.9289 | 1.4132E-06 | 4.9482 |
| | 1/32 | 3.4489E-06 | 3.9670 | 7.6709E-10 | 6.0935 | 1.8865E-06 | 3.9648 | 4.5777E-08 | 4.9743 |
| | 1/64 | 2.2054E-07 | 3.9840 | 1.1234E-11 | 6.0273 | 1.2082E-07 | 3.9825 | 1.4563E-09 | 4.9872 |

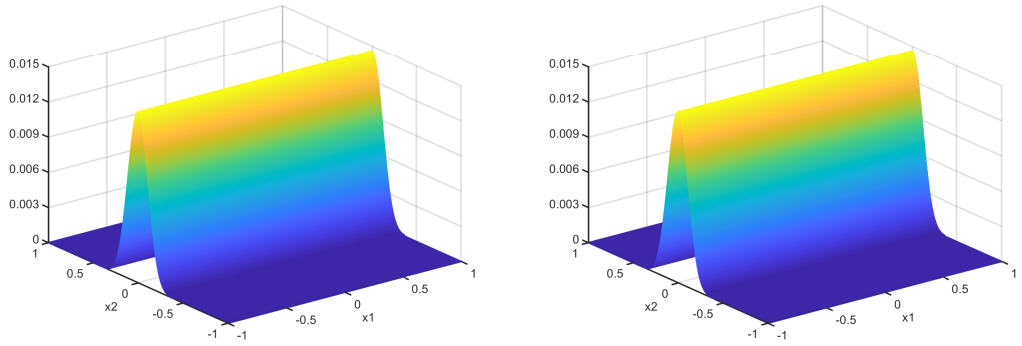


**(a)** $t = 0$ **(b)** $t = 1$

**Figure 6.** The plotting of exact solutions at the initial and final times for Example 5.2 with $z = 6.1$ and Dirichlet BC.

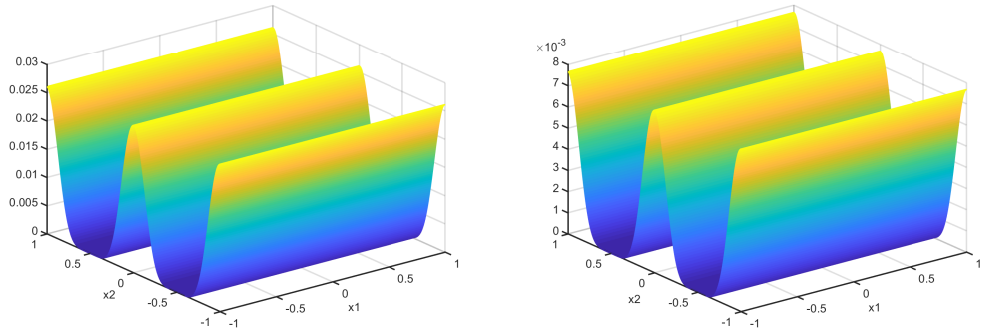


**(a)** $t = 0$ **(b)** $t = 1$

**Figure 7.** The plotting of exact solutions at the initial and final times for Example 5.2 with $z = 6.1$ and Neumann BC.

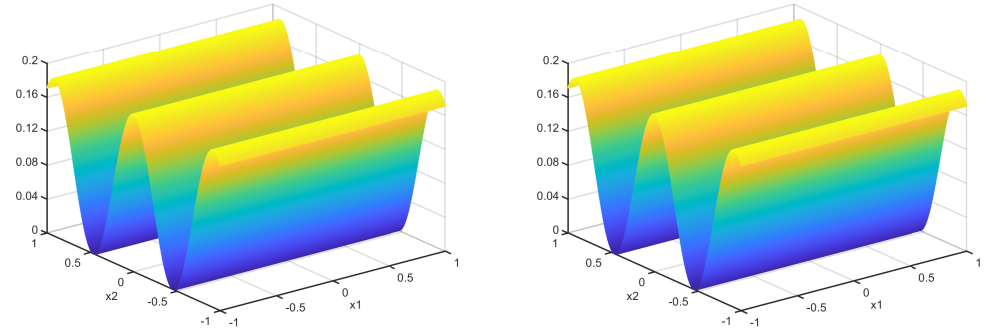


**(a)** $t = 0$ **(b)** $t = 1$

**Figure 8.** The plotting of exact solutions at the initial and final times for Example 5.2 with $z = 6.1$ and Robin BC.

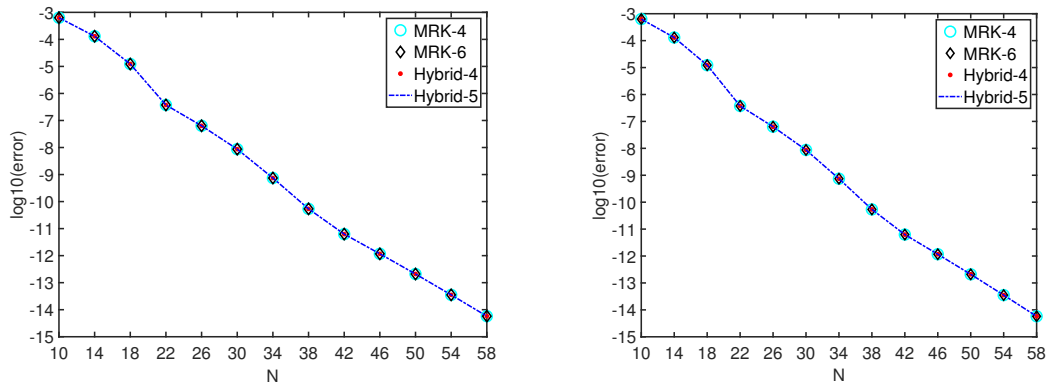


**(a)** $\alpha = 1.2$ **(b)** $\alpha = 1.8$

**Figure 9.** Errors and convergence rates in space for Example 5.2 with $\nu = \alpha^{-3}$, $t = 1$, $t_0 = 0.5$, $z = 6.1$, $\tau = \frac{1}{5000}$, and Dirichlet BC.

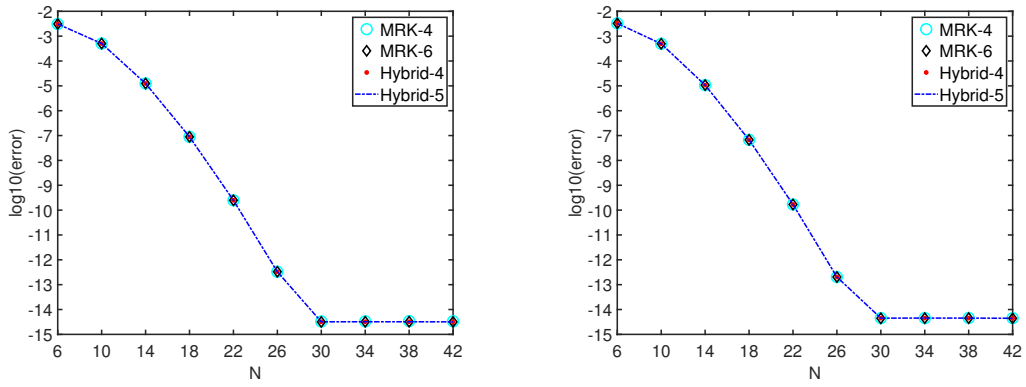


**(a)** $\alpha = 1.2$ **(b)** $\alpha = 1.8$

**Figure 10.** Errors and convergence rates in space for Example 5.2 with $\nu = 2\alpha^{-4}$, $t = 1$, $t_0 = 0.55$, $z = 6.1$, $\tau = \frac{1}{5000}$, and Neumann BC.

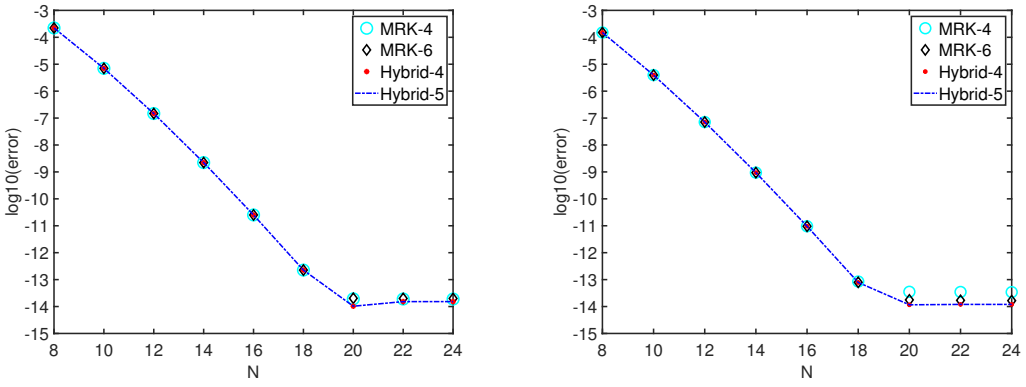


**(a)** $\alpha = 1.2$ **(b)** $\alpha = 1.8$

**Figure 11.** Errors and convergence rates in space for Example 5.2 with $\nu = \alpha^{-1}$, $t = 1$, $t_0 = 0.5$, $z = 6.1$, $\tau = \frac{1}{5000}$, and Robin BC.

**Example 5.3** (3-dimensional)**.** *Consider NSFDE (1.1) with* $d = 3$*, Neumann BC,* $u_0(\boldsymbol{x}) = (-t_0)^z \cos(\pi(x_1 + 1)) \cos(\pi(x_2 + 1)) \cos(\pi(x_3 + 1))$*, and*

$$\begin{aligned} f(u(\boldsymbol{x}), \boldsymbol{x}, t) =& z(t - t_0)^{z-1} \cos(\pi(x_1 + 1)) \cos(\pi(x_2 + 1)) \cos(\pi(x_3 + 1)) \\ &+ \nu(t - t_0)^z (3\pi^2)^{\frac{\alpha}{2}} \cos(\pi(x_1 + 1)) \cos(\pi(x_2 + 1)) \cos(\pi(x_3 + 1)) \\ &+ u(\boldsymbol{x}, t)^2 - (t - t_0)^{2z} [\cos(\pi(x_1 + 1)) \cos(\pi(x_2 + 1)) \cos(\pi(x_3 + 1))]^2. \end{aligned}$$

*The corresponding exact solution is* $u(\boldsymbol{x}, t) = (t - t_0)^z \cos(\pi(x_1 + 1)) \cos(\pi(x_2 + 1)) \cos(\pi(x_3 + 1))$.

From Table 4 and Figure 12, we observe the convergence rates in time and space in agreement with the estimate in Theorem 4.3, which shows our numerical method and theoretical estimates are valid for high-dimensional problem.

**Table 4.** Errors and convergence rates in time for Example 5.3 with Neumann BC, $z = 6.1$, $\nu = 2a^{-4}$, $N = 20$, $t_0 = 1/3$, and $t = 1$.

| $\alpha$ | $\tau$ | MRK4 | | MRK6 | | Hybrid-4 | | Hybrid-5 | |
|---|---|---|---|---|---|---|---|---|---|
| | | $L^2$-error | rate | $L^2$-error | rate | $L^2$-error | rate | $L^2$-error | rate |
| | 1/8 | 4.1535E-04 | 3.7674 | 5.3057E-06 | 5.7243 | 1.1052E-04 | 3.8489 | 1.0531E-05 | 4.8992 |
| 1.2 | 1/16 | 3.0501E-05 | 3.8950 | 1.0036E-07 | 5.8671 | 7.6702E-06 | 3.9294 | 3.5292E-07 | 4.9535 |
| | 1/32 | 2.0502E-06 | 3.9506 | 1.7195E-09 | 5.9346 | 5.0342E-07 | 3.9660 | 1.1390E-08 | 4.9777 |
| | 1/64 | 1.3260E-07 | 3.9761 | 2.8114E-11 | 5.9581 | 3.2215E-08 | 3.9833 | 3.6148E-10 | 4.9894 |
| | 1/8 | 2.0945E-04 | 3.8291 | 1.4343E-06 | 5.8094 | 8.2325E-05 | 3.8856 | 7.9558E-06 | 4.9083 |
| 1.8 | 1/16 | 1.4737E-05 | 3.9209 | 2.5577E-08 | 5.9050 | 5.5700E-06 | 3.9456 | 2.6494E-07 | 4.9566 |
| | 1/32 | 9.7301E-07 | 3.9621 | 4.2684E-10 | 5.9529 | 3.6149E-07 | 3.9735 | 8.5323E-09 | 4.9790 |
| | 1/64 | 6.2432E-08 | 3.9815 | 6.8905E-12 | 5.9382 | 2.3012E-08 | 3.9869 | 2.7054E-10 | 4.9900 |

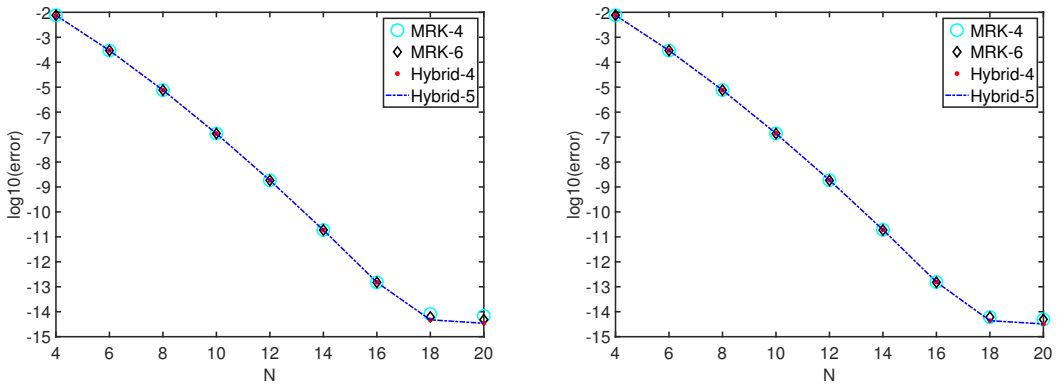


**(a)** $\alpha = 1.2$ **(b)** $\alpha = 1.8$

**Figure 12.** Errors and convergence rates in space for Example 5.3 with $\nu = 2a^{-4}$, $t = 1$, $t_0 = 1/3$, $z = 6.1$, $\tau = \frac{1}{5000}$, and Neumann BC.

**Example 5.4.** *Finally, we consider NSFDE (1.1) with Neumann BC,* $u(x, 0) = \frac{1}{2}\sin(\frac{3\pi x}{2})(\cos(\pi x) - 1)$, $x \in (-1, 1)$, *and* $f(u(x, t), \boldsymbol{x}, t) = u(x, t)(1 - u(x, t)^2)$,

The Example 5.4 is usually called the fractional Allen-Cahn equation, which is widely employed to describe the formation and evolution of phase boundaries with nonlocal effects. The interfacial characteristics of the Allen-Cahn equation were analyzed in [52, 53], which demonstrated that a decrease in $\alpha$ leads to a more rapid variation of the solution near the interface center, while farther from the center, the profiles flatten and the whole interface thickens. Here, we study the effect of fractional diffusion on the metastability of the solutions. From the first case in Figure 13, which is the classical Allen-Cahn equation (i.e., $\alpha = 2$), it shows that the initial configuration evolves into an intermediate unstable state and then quickly changes into a single-interface pattern. As $\alpha$ is decreasing,

the lifetime of the unstable interface is significantly extended and eventually becomes fully stabilized, which results in the nonlocal influence of the fractional Laplacian.

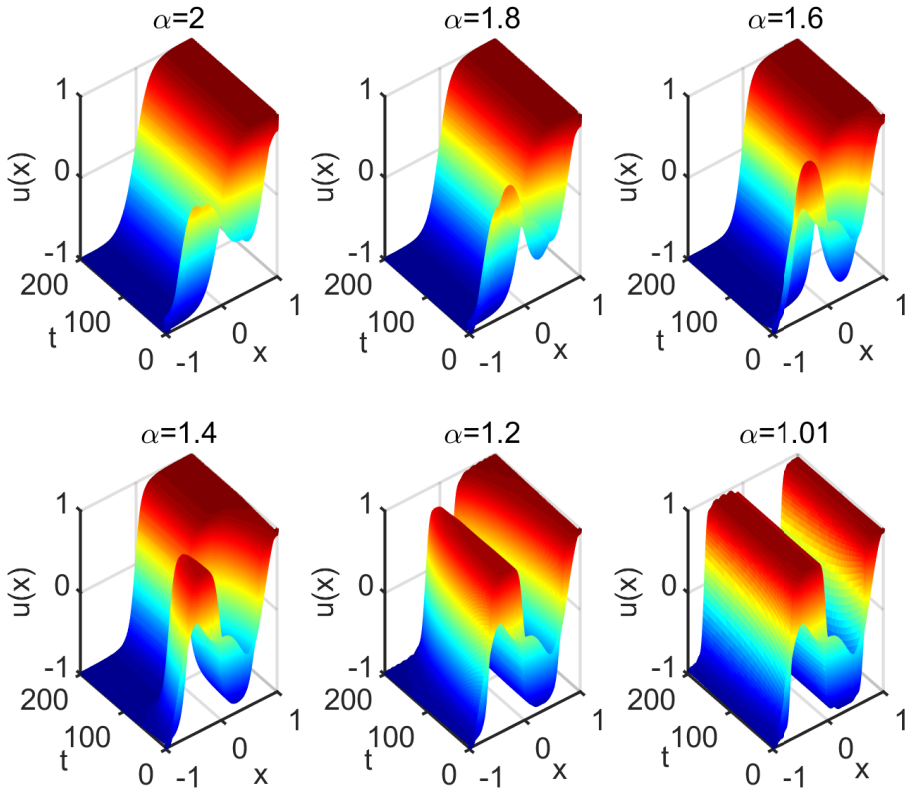


**(a)**

**Figure 13.** Numerical simulation for Example 5.4 with MRK6, $\nu = 0.03$, $N = 40$, and $\tau = \frac{1}{20000}$.

## 6. Conclusions

We have developed a high-order algorithm with matched temporal and spatial accuracy for the nonlinear space-fractional diffusion equation that characterizes the fractional random walk dynamics on a network. The numerical scheme combines a spectral Galerkin method employing a Fourier-like basis in space and general linear methods in time. We give the solvability of the numerical scheme when the nonlinear term fulfills the locally Lipschitz condition. Under $(k, l)$-algebraic stability, we prove that the proposed method is stable, and its temporal convergence rate is equal to the general stage order of the general linear method. In addition, we derive the error estimate is space, in which the convergence rate is optimal and independent of the fractional parameter $\alpha$. Finally, some numerical examples further confirm the accuracy and computational efficiency of the proposed method.

## Use of AI tools declaration

The authors declare they have not used Artificial Intelligence (AI) tools in the creation of this article.

## Acknowledgments

This work is supported by the Natural Science Foundation of Hunan Province, China (Grant No. 2025JJ60044), the Natural Science Foundation of Heilongjiang Province, China (Grant No. PL2024A002), the Natural Science Foundation of Zhejiang Province, China (Grant No. LQ21A010007), the Scientific Research Fund of Hunan Provincial Education Department (Grant No. 22B0879).

## Conflict of interest

The authors declare there is no conflict of interest.

## References

1. D. Brockmann, L. Hufnagel, T. Geisel, The scaling laws of human travel, *Nature*, **439** (2006), 462–465. https://doi.org/10.1038/nature04292
2. M. B. A. Barrat, A. Vespignani, *Dynamical Processes on Complex Networks*, Cambridge University Press, 2013.
3. W. Huang, S. Chen, W. Wang, Navigation in spatial networks: A survey, *Physica A*, **393** (2014), 132–154. https://doi.org/10.1016/j.physa.2013.09.014
4. T. Michelitsch, A. P. Riascos, B. Collet, A. Nowakowski, F. Nicolleau, *Fractional Dynamics on Networks and Lattices*, John Wiley & Sons, 2019. https://doi.org/10.1002/9781119608165
5. J. D. Noh, H. Rieger, Random walks on complex networks, *Phys. Rev. Lett.*, **92** (2004), 118701. https://doi.org/10.1103/PhysRevLett.92.118701
6. S. N. Dorogovtsev, A. V. Goltsev, J. F. Mendes, Critical phenomena in complex networks, *Rev. Mod. Phys.*, **80** (2008), 1275–1335. https://doi.org/10.1103/RevModPhys.80.1275
7. Z. Zhang, A. Julaiti, B. Hou, H. Zhang, G. Chen, Mean first-passage time for random walks on undirected networks, *Eur. Phys. J. B*, **84** (2011), 691–697. https://doi.org/10.1140/epjb/e2011-20834-1
8. A. P. Riascos, J. L. Mateos, Long-range navigation on complex networks using lévy random walks, *Phys. Rev. E*, **86** (2012), 056110. https://doi.org/10.1103/PhysRevE.86.056110
9. T. Michelitsch, B. Collet, A. P. Riascos, A. Nowakowski, F. Nicolleau, Recurrence of random walks with long-range steps generated by fractional laplacian matrices on regular networks and simple cubic lattices, *J. Phys. A: Math. Theor.*, **50** (2017), 505004. https://doi.org/10.1088/1751-8121/aa9008
10. T. M. Michelitsch, B. Collet, A. P. Riascos, A. Nowakowski, F. C. Nicolleau, Fractional random walk lattice dynamics, *J. Phys. A: Math. Theor.*, **50** (2017), 055003. https://doi.org/10.1088/1751-8121/aa5173

11. A. P. Riascos, J. L. Mateos, Fractional dynamics on networks: Emergence of anomalous diffusion and lévy flights, *Phys. Rev. E*, **90** (2014), 032809. https://doi.org/10.1103/PhysRevE.90.032809

12. A. Riascos, J. L. Mateos, Fractional diffusion on circulant networks: emergence of a dynamical small world, *J. Stat. Mech: Theory Exp.*, **2015** (2015), P07015. https://doi.org/10.1088/1742-5468/2015/07/P07015

13. Y. Zhang, D. A. Benson, D. M. Reeves, Time and space nonlocalities underlying fractional-derivative models: Distinction and literature review of field applications, *Adv. Water Resour.*, **32** (2009), 561–581. https://doi.org/10.1016/j.advwatres.2009.01.008

14. C. Lee, Y. Nam, M. Bang, S. Ham, J. Kim, Numerical investigation of the dynamics for a normalized time-fractional diffusion equation, *AIMS Math.*, **9** (2024), 26671–26687. https://doi.org/10.3934/math.20241297

15. S. Duo, L. Ju, Y. Zhang, A fast algorithm for solving the space-time fractional diffusion equation, *Comput. Math. Appl.*, **75** (2018), 1929–1941. https://doi.org/10.1016/j.camwa.2017.04.008

16. Z. Hao, Z. Zhang, R. Du, Fractional centered difference scheme for high-dimensional integral fractional Laplacian, *J. Comput. Phys.*, **424** (2021), 109851. https://doi.org/10.1016/j.jcp.2020.109851

17. M. Zhang, F. Liu, I. W. Turner, V. V. Anh, A vertex-centred finite volume method for the 3d multi-term time and space fractional bloch–torrey equation with fractional Laplacian, *Commun. Nonlinear Sci. Numer. Simul.*, **114** (2022), 106666. https://doi.org/10.1016/j.cnsns.2022.106666

18. C. Sheng, B. Su, C. Xu, Efficient monte carlo method for integral fractional laplacian in multiple dimensions, *SIAM J. Numer. Anal.*, **61** (2023), 2035–2061. https://doi.org/10.1137/22M1504706

19. C. Jiao, C. Li, Monte carlo method for parabolic equations involving fractional Laplacian, *Monte Carlo Methods Appl.*, **29** (2023), 33–53. https://doi.org/10.1515/mcma-2022-2129

20. B. Yin, Y. Liu, H. Li, S. He, Fast algorithm based on tt-m fe system for space fractional allen–cahn equations with smooth and non-smooth solutions, *J. Comput. Phys.*, **379** (2019), 351–372. https://doi.org/10.1016/j.jcp.2018.12.004

21. R. H. Nochetto, E. Otárola, A. J. Salgado, A PDE approach to fractional diffusion in general domains: a priori error analysis, *Found. Comput. Math.*, **15** (2015), 733–791. https://doi.org/10.1007/s10208-014-9208-x

22. L. Chen, R. Nochetto, E. Otárola, A. Salgado, Multilevel methods for nonuniformly elliptic operators and fractional diffusion, *Math. Comput.*, **85** (2016), 2583–2607. https://doi.org/10.1090/mcom/3089

23. A. Bonito, W. Lei, J. E. Pasciak, On sinc quadrature approximations of fractional powers of regularly accretive operators, *J. Numer. Math.*, **27** (2019), 57–68. https://doi.org/10.1515/jnma-2017-0116

24. A. Bueno-Orovio, D. Kay, K. Burrage, Fourier spectral methods for fractional-in-space reaction-diffusion equations, *BIT Numer. Math.*, **54** (2014), 937–954. https://doi.org/10.1007/s10543-014-0484-2

25. F. Song, C. Xu, G. E. Karniadakis, Computing fractional laplacians on complex-geometry domains: algorithms and simulations, *SIAM J. Sci. Comput.*, **39** (2017), A1320–A1344. https://doi.org/10.1137/16M1078197
26. T. Tang, L. Wang, H. Yuan, T. Zhou, Rational spectral methods for PDEs involving fractional Laplacian in unbounded domains, *SIAM J. Sci. Comput.*, **42** (2020), A585–A611. https://doi.org/10.1137/19M1244299
27. H. Zhang, X. Jiang, F. Zeng, G. E. Karniadakis, A stabilized semi-implicit fourier spectral method for nonlinear space-fractional reaction-diffusion equations, *J. Comput. Phys.*, **405** (2020), 109141. https://doi.org/10.1016/j.jcp.2019.109141
28. S. Chen, J. Shen, L. L. Wang, Generalized Jacobi functions and their applications to fractional differential equations, *Math. Comput.*, **85** (2016), 1603–1638. https://doi.org/10.1090/mcom3035
29. C. Sheng, D. Cao, J. Shen, Efficient spectral methods for PDEs with spectral fractional Laplacian, *J. Sci. Comput.*, **88** (2021), 4. https://doi.org/10.1007/s10915-021-01491-2
30. C. Sheng, J. Shen, T. Tang, L. L. Wang, H. Yuan, Fast fourier-like mapped chebyshev spectral-galerkin methods for pdes with integral fractional laplacian in unbounded domains, *SIAM J. Numer. Anal.*, **58** (2020), 2435–2464. https://doi.org/10.1137/19M128377X
31. C. Sheng, S. Ma, H. Li, L. L. Wang, L. Jia, Nontensorial generalised hermite spectral methods for pdes with fractional laplacian and schrödinger operators, *ESAIM. Math. Model. Numer. Anal.*, **55** (2021), 2141–2168. https://doi.org/10.1051/m2an/2021049
32. J. Burkardt, Y. Wu, Y. Zhang, A unified meshfree pseudospectral method for solving both classical and fractional PDEs, *SIAM J. Sci. Comput.*, **43** (2021), A1389–A1411. https://doi.org/10.1137/20M1335959
33. D. Nie, W. Deng, Local discontinuous galerkin method for the fractional diffusion equation with integral fractional laplacian, *Comput. Math. Appl.*, **104** (2021), 44–49. https://doi.org/10.1016/j.camwa.2021.11.007
34. W. Wang, Y. Huang, J. Tang, Lie-Trotter operator splitting spectral method for linear semiclassical fractional Schrödinger equation, *Comput. Math. Appl.*, **113** (2022), 117–129. https://doi.org/10.1016/j.camwa.2022.03.016
35. W. Wang, Y. Huang, Analytical and numerical dissipativity for the space-fractional Allen–Cahn equation, *Math. Comput. Simul.*, **207** (2023), 80–96. https://doi.org/10.1016/j.matcom.2022.12.012
36. B. Yu, X. Zheng, P. Zhang, L. Zhang, Computing solution landscape of nonlinear space-fractional problem via fast approximation algorithm, *J. Comput. Phys.*, **468** (2022), 111513. https://doi.org/10.1016/j.jcp.2022.111513
37. Y. Xu, Y. Zhang, J. Zhao, Backward difference formulae and spectral Galerkin methods for the Riesz space fractional diffusion equation, *Math. Comput. Simul.*, **166** (2019), 494–507. https://doi.org/10.1016/j.matcom.2019.07.007
38. Y. Zhang, Y. Li, Y. Yu, W. Wang, Implicit Runge-Kutta with spectral Galerkin methods for the fractional diffusion equation with spectral fractional Laplacian, *Numer. Methods Partial Differ. Equations*, **40** (2024), e23074. https://doi.org/10.1002/num.23074

39. J. C. Butcher, General linear methods, *Acta Numer.*, **15** (2006), 157–256. https://doi.org/10.1017/S0962492906220014
40. K. Burrage, J. C. Butcher, Non-linear stability of a general class of differential equation methods, *BIT Numer. Math.*, **20** (1980), 185–203. https://doi.org/10.1007/BF01933191
41. S. Li, Stability and B-convergence of general linear methods, *J. Comput. Appl. Math.*, **28** (1989), 281–296. https://doi.org/10.1016/0377-0427(89)90340-3
42. S. Li, *Numerical Analysis for Stiff Ordinary and Functional Differential Equations*, Xiangtan University Publisher, 2010.
43. J. Shen, L. L. Wang, Fourierization of the Legendre–Galerkin method and a new space–time spectral method, *Appl. Numer. Math.*, **57** (2007), 710–720. https://doi.org/10.1016/j.apnum.2006.07.012
44. V. J. Ervin, J. P. Roop, Variational solution of fractional advection dispersion equations on bounded domains in $\mathbb{R}^d$, *Numer. Methods Partial Differ. Equations*, **23** (2007), 256–281. https://doi.org/10.1002/num.20169
45. E. Hairer, G. Wanner, *Solving Ordinary Differential Equations II—Stiff and Differential-Algebraic Problems*, Springer Verlag, Berlin, 1996. https://doi.org/10.1007/978-3-642-05221-7
46. C. Huang, Q. Chang, A. Xiao, B-convergence of general linear methods for stiff problems, *Appl. Numer. Math.*, **47** (2003), 31–44. https://doi.org/10.1016/S0168-9274(03)00051-5
47. Y. Xu, Y. Zhang, J. Zhao, General linear and spectral Galerkin methods for the Riesz space fractional diffusion equation, *Appl. Math. Comput.*, **364** (2020), 124664. https://doi.org/10.1016/j.amc.2019.124664
48. S. Li, Stability and B-convergence properties of multistep Runge-Kutta methods, *Math. Comput.*, **69** (2000), 1481–1504. https://doi.org/10.1090/S0025-5718-99-01159-X
49. Y. Zhang, Y. Fan, Y. Li, General linear and spectral Galerkin methods for the nonlinear two-sided space distributed-order diffusion equation, *Comput. Math. Appl.*, **113** (2022), 1–12. https://doi.org/10.1016/j.camwa.2022.03.021
50. Y. Zhang, Y. Li, Y. Yu, W. Wang, Error estimates of general linear and spectral galerkin methods for the fractional diffusion equation with spectral fractional Laplacian, *Comput. Appl. Math.*, **44** (2025), 157. https://doi.org/10.1007/s40314-025-03116-y
51. D. S. Grebenkov, B. T. Nguyen, Geometrical structure of Laplacian eigenfunctions, *SIAM Rev.*, **55** (2013), 601–667. https://doi.org/10.1137/120880173
52. K. Burrage, N. Hale, D. Kay, An efficient implicit FEM scheme for fractional-in-space reaction–diffusion equations, *SIAM J. Sci. Comput.*, **34** (2012), A2145–A2172. https://doi.org/10.1137/110847007
53. C. Lee, S. Ham, Y. Hwang, S. Kwak, J. Kim, An explicit fourth-order accurate compact method for the allen-cahn equation, *AIMS Math.*, **9** (2024), 735–762. https://doi.org/10.3934/math.2024038



AIMS Press